Cytokine-Detecting Biosensor: Covalently Functionalizing Surfaces with Aptamers for Reusable and Fast Detection of Small Proteins

by

Yue Ling

A THESIS SUBMITTED IN PARTIAL FULFILLMENT OF THE REQUIREMENTS FOR THE DEGREE OF BACHELOR OF APPLIED SCIENCE

in the

School of Engineering Science

SIMON FRASER UNIVERSITY

Fall 2020

APPROVAL

Name: Eric (Yue) Ling

Degree: Bachelor of Applied Science (Honours)

Title of Thesis: Cytokine-Detecting Biosensor: Covalently Functionalizing Surfaces with Aptamers for Reusable and Fast Detection of Small Proteins

Dr. Glenn Chapman, P.Eng
Director, School of Engineering Science

Examining Committee:

Dr. Michael Adachi, P.Eng (Supervisor and Chair)
Assistant Professor, School of Engineering Science

Dr. Karen Kavanagh
Professor, Dept. of Physics

Dr. Ash M. Parameswaran, P. Eng.
Professor, School of Engineering Science

Date Approved: Nov. 30th, 2020

Abstract

This thesis outlines a modular method to covalently functionalized surfaces with aptamers to sense for small proteins. Small proteins, such as cytokines, are related to a variety of diseases such as Rheumatoid arthritis, cancer, Alzheimer's, eczema, etc. Current methods for detecting these small proteins are antibody-based single-use systems requiring specialized skills, long incubation times, and expensive equipment. We propose a method of aptamer-based biosensing that would be reusable, more versatile, and offer simpler operations.

Aptamers are synthetic chains of nucleotides made in vitro selection (SELEX) through repeated purification and washing cycles that provide the ability to bind tightly to any target. Aptamers capture target molecules via hydrogen-bond interactions, which are weaker than the covalent bonds between aptamers and the sensor base surface. Using this characteristic, the biosensing layer can be reused by breaking the hydrogen-bonds with a high concentration urea wash. Such a treatment will destroy antibody-based biosensors but can be sustained by aptamers.

Atomic-layer-deposition (ALD) of silica onto stable surfaces enables surface functionalization. The deposited silica allows silane chemistry functionalization, as well as passivates and protects underlying fragile 2D TMD surfaces. By immobilizing specific aptamers to a silica surface via silane chemistry, users can measure the mass change and/or fluorescence difference upon target attachment on the silica substrates.

Optical detection of proteins involves constructing a partial-complementary loopback-structured fluorescent dye-labeled aptamer. Upon aptamer binding with the higher binding-affinity target, the aptamer will deform and move the fluorescent dye to a different position. The deformation results in a fluorescence intensity change that could indicate a target protein binding.

A quartz crystal microbalance (QCM) is an acoustic sensor that can measure a material's resonant vibration frequency. A material's resonant frequency is correlated to its mass. By immobilizing aptamers onto QCM silica quartz crystal surfaces, the added mass of a target bounded by the aptamers can be sensed by a change in resonant frequency. With an increasing amount of target proteins, TNF Alpha (TNFa), interacted with the biosensor, a corresponding decrease in resonant vibration frequency is measured. Non-target cytokines, Interferon Gamma (IFNg), were introduced to the QCM to test the biosensing sensitivity. For the same concentration of IFNg and TNFa, only the TNFa interaction elicited a decrease in resonance vibration frequency. The proposed biosensor was able to obtain high selectivity and reusability.

Applications of functionalized TMD (ft-TMD) or general surfaces include target medicine, target therapy, acoustic wave, fluorescent, and electrochemical sensors. This thesis explores the design and sensing of the proposed reusable and target-generalizable sensing layer.

Keywords: Aptamers; Quartz Crystal Microbalance; Covalent Functionalization; Reusable; Cytokine; Early Disease Detection

Acknowledgments

I would like to thank my supervisor, Dr. Michael Adachi, for his continued support and the leap of faith he took in me for this growing, invigorating, and interesting project. Michael's guidance and discerning insights allowed the project to progress even when experiments didn't go as well as planned. I am really grateful for Dr. Adachi's buying so many experiment material and characterization tools. The nurturing and collaborative environment Professor Adachi harboured at SFU Nanodevice and Fabrication Group is very fertile and growth-inducing. Lab members: Amin Abnavi, Samantha Betts, Mirette Fawzy, Thushani De Silva, and Bennett Sasaki are always eager to help each other out and try to hash out the best "next steps". I am most thankful for Dr. Adachi's unwavering patience, kindness, and openness to my many questions and failures throughout the whole project.

Dr. Adachi also introduced us to very resourceful and experienced researchers: Dr. Miriam Rosin from Biomedical Physiology and Kinesiology and Dr. Karen Kavanagh from Physics, both of whom gave very insightful and vibrant feedback and ideas to the project. I am thankful for their introducing me to aptamers and constructive criticisms.

I would like to thank Dr. Tyler Cuthbert, Mandeep Kaur, and Dr. Carlo Menon for allowing me to work in the Polymer Lab and generously sharing some resources. I am extremely grateful for all the help Dr. Tyler Cuthbert has given me in the lab: experiment design, data analysis, and communication. Dr. Cutherbert's teaching about chemical reactions, characterization, brainstorming, and algorithm development has broadened my perspectives.

I am grateful to Dr. Wen Zhou from Chemistry for showing me how to use Chemistry's characterization equipment and brainstorming with me about characterization methods. I am also thankful for Science Stores' David Lee for helping us pick out our equipment and for taking us across many biology labs to look for a small centrifuge. I am thankful to Kun Liu and Prince Lat's fluorescent and radiation imaging advice and lab help. I would also like to thank Matthew Brown for training me to use the Raman machine. I would also like to thank Dr. Peter Unran's radioisotope labeling characterization idea we discussed.

I would like to give a special thanks to my thesis committee, Dr. Ash Parameswaran and Dr. Karen Kavanagh for taking time out to read my thesis documents, giving me a thorough proofreading, and encouraging comments. I am grateful to Dr. Ash's lending me his freezer and laser and especially thankful for Karen's allowing me to work in her lab during these COVID-19 lab-restrictive times.

I would like to thank my friends and family for their continued support and advice along the way. I feel extremely lucky to be surrounded by so many supportive and loving individuals. This sense of community made going through engineering more colourful and fun.

Table of Contents

List of Tables

List of Figures

List of Acronyms

Acronym	Definition
ALD	Atomic Layer Deposition
apt	Aptamer
aptabeacons	Aptamer Beacons
aptasensor	Aptamer Sensors
ATR-FTIR	Attenuated Total Reflectance-Fourier Transform Infrared Spectroscopy
BSA	Bovine Serum Albumin
CDI	Carbonyldiimidazole
cyt	Cytokine
FRET	Förster Resonance Energy Transfer
ft-TMD	Functionalized Transition Metal Dichalcogenides
GOPS	(Glycidoxypropyl)Trimethoxysilane
HCl	Hydrochloric Acid
IFNg	Interferon Gamma
PBS	Phosphate Buffered Saline (pH 7.4)
QCM	Quartz Crystal Microbalance
SELEX	Systemic Evolution Of Ligands By Exponential Enrichment
SEM-EDX	Scanning Electron Microscopy - Energy Dispersive X-Ray Spectroscopy
TGA	Thermogravimetric Analysis
TMD	Transition Metal Dichalcogenides
TNFa	Tumour Necrosis Factor Alpha
XPS	X-Ray Photoelectron Spectroscopy

Chapter 1: Introduction

Transition Metal Dichalcogenides (TMD) are piezoelectric materials that change their electronic properties corresponding to changes in mechanical stress and vice versa [1]. TMDs are used to build highly sensitive acoustic wave sensors that change their resonant frequency in response to differing mass bounded on the surface [2]. When acoustic wave sensor surfaces are functionalized with aptamers, one will be able to accurately detect target molecules.

Aptamers are nucleotide-based proteins that have high specificity and affinity to any given target via in vitro selection of these targets [3][4][5]. Aptamers are made by systemic evolution of ligands by exponential enrichment (SELEX), a process which involves washing and isolating the target-bounded oligonucleotides and amplifying such oligonucleotides, and repeating the process until a high target-affinity oligonucleotides chain is created [6]. The benefit of aptamers over antibodies is the ability to withstand harsh environments and revert denatured states. With the use of either heat, salt concentration, chelating agents, chaotropic agents, or protein denaturants (guanidinium hydrochloride or Urea) to break the target-aptamer bond, the aptamer sensing layer can be recovered and used for subsequent measurements [6][7].

When aptamers are covalently attached to Quartz Crystal Microbalance (QCM) crystals, TMD surfaces, or other mechanisms' surfaces, one can accurately detect target molecules. Without aptamers or other target-capturing molecules (such as antibodies), the sensing surfaces would not be specific to the target molecule, which will lead to false positives. Figure 1 shows an overview graphical representation of a biosensor.

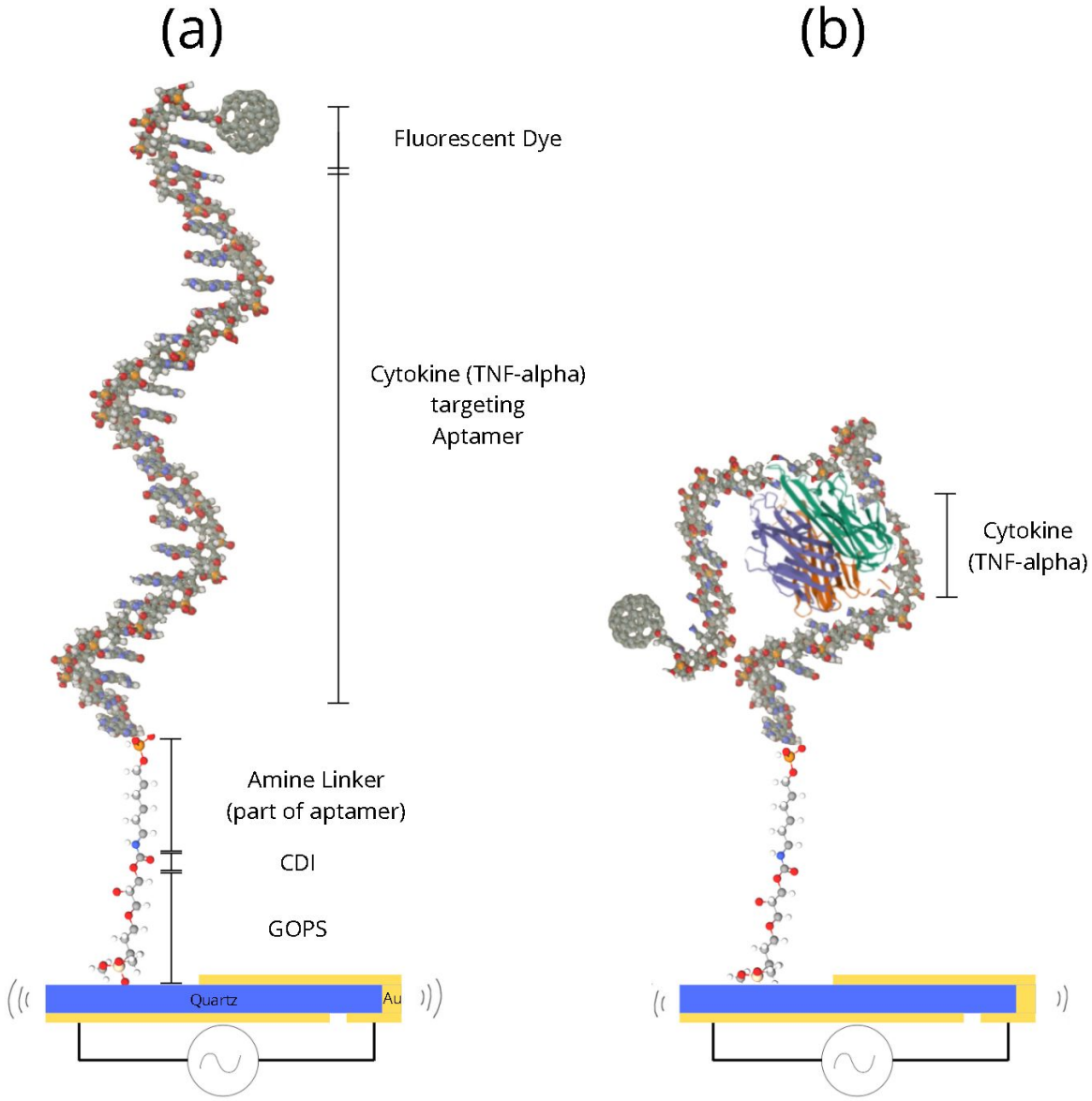

Figure 1: Overview Representation of the Biosensor. (a) shows the upright aptamer orientation when no cytokine bounded. The resonance vibration frequency is higher in (a) than (b) because of a lower mass bounded on the surface as illustrated by the fewer vibrational lines beside the QCM crystal. (b) shows aptamer shape deformation bending inwards when cytokine is bounded. This shape deformation will dim the fluorescence intensity.

1.1 Current Cytokine Detection Methods

Cytokines are inflammatory proteins in our body that are related to a majority of diseases including cancer, HIV, Rheumatoid Arthritis, Atherosclerosis, and Alzheimer's [3][8][9]. Abnormal levels of cytokine concentration in the body correlate with inflammatory diseases [4][8][9].

Cytokines play a regulatory role in maintaining “host defense and normal and abnormal homeostatic mechanism” [10]. Cytokines may trigger or terminate inflammatory responses by exerting, directly or via other cells, crytodestructive effects on infection agents or tumour cells [10]. Detecting such proteins are useful for early disease diagnosis and as a measurement of the effectiveness of new treatment such as gene therapy.

Current technologies for cytokine detection employ enzyme-linked immunosorbent assay (ELISA) immunoassays, which is expensive (equipment and reagents requirement), labour and time-intensive (6 hours per cytokine sample measurement), and single-use [4][11][12]. Another method for small protein detection is using antibody-based proximity ligation where samples of small proteins are incubated with proximity probes, connector, ligase, and Polymerase chain reaction (PCR) components [13]. The proximity and target proteins reactions are then transferred into PCR instruments for temperature cycling. In total, the proximity ligation method consumes more than 3 hours and requires incubators and expensive PCR machines [13]. A real-time and multi-use detection biosensor of cytokines can decrease the associated costs and improve infectious disease monitoring and/or detection.

1.2 Current Aptamer-based Sensors

Aptamer-based biosensors for detecting small proteins are favourable over antibody-based biosensors because of their resistance to denaturing conditions, longer shelf life, cheaper costs, and harmlessness [14]. Some notable aptamer-based detector types are: electrochemical, optical (fluorescence/ colorimetry), and mass-sensitive [3][5][15][16][17]. Depending on the functionalization method, some of these sensors are reusable but require highly reactive and toxic chemical reactions [18]. Other reusable functionalizing methods require expensive linkers to induce covalent interactions and/ or bonds on specific surfaces such as gold or TMDs with sulfur vacancies [19]. Some functionalizing methods are simply single-use (like antibody-based) and do not reap the full benefit of using urea-resilient aptamers [5][16][20][21]. The ideal aptamer-based biosensor is reusable, has high detection sensitivity and specificity, made of lower toxicity material, functionalizable on a wide range of surfaces, and employs easy measuring techniques.

Chapter 2: Development Roadmap

The purpose of the project is to make a reusable, mass sensitive or optical aptamer-based biosensor using relatively harmless and inexpensive material.

2.1 Different Functionalization Methods: Choosing Covalent Functionalization

Functionalizing TMD surfaces directly is difficult because TMD 2H-phase is highly stable. Using n-butyl lithium and subsequent reaction with water creates the more reactive surface of 1T

phase TMD [18][22]. The 1T-MoS_2 phase TMD was described to be able to react with organoiodides or diazonium salt creating covalent bonds. However, this method was ultimately forfeited because of the use of n-butyl lithium, which is quite a hazardous chemical. In addition, 1T-MoS_2 no longer has piezoelectric properties, a desirable trait in 2H-MoS_2 useful in creating a sensitive biosensor.

Coordination chemistry of the sensing layer surface would involve interacting the 2H TMD monolayer with coordinated metal-acetate [22][23]. The methods commonly used involving Copper (II), Nickel (II), or Zinc (II) acetate are fairly hazardous. Copper (I) acetate is the least toxic; however, coordination chemistry ultimately does not produce bonds as strong as covalent bonds [23]. Other types of covalent bonds involve both atoms to create the bond, whereas coordination covalent bonds are supplied by one atom. If the bond affinity of the coordinate covalent bond is greater than aptamer to target, this method could still work for a reusable biosensing layer. As a result of the potentially weaker bond created, the coordinate bond method was chosen as a back-up method.

Self-assembled monolayer (SAM), electrostatic, and physisorbed methods are fairly similar and rely on van der waals (VDW) forces, which is not ideal for reusable devices. Surfaces are often doped and tuned to change their surface electrical, optical, mechanical, or magnetic properties [24][25]. Some devices simply soak the surface in a buffer solution with aptamer, which merely creates single-use devices [16]. Because of the weak bonds between aptamers and the sensing surface, when rinsing off-target cytokine molecules with 7M urea, the physisorbed aptamer would also be rinsed off and cannot be reused for subsequent detection.

Covalent functionalization is the preferred method because of the strong bonds between the aptamers and the biosensor substrate surface, ideal for reusable biosensors. Among the many covalent methods, silane chemistry with Glycidoxypropyltrimethoxysilane (GOPS) interacted with Carbonyldiimidazole (CDI) uses the least toxic chemicals and are cheaper than other more toxic alternatives [7][25][26]. The modified surface would then be able to form a covalent bond with amine-terminated aptamers. In addition, the use of silica is highly beneficial because of the lower cost and wide usage of silica in integrated circuits (IC) technology: silica could potentially provide easier and cheaper integration with other electronics. Surfaces can also be easily modified to be coated with silica by using atomic layer deposition (ALD) enabling many different surface materials to become biosensing layers [27]. Aside from all the advantages of covalent functionalization with silane chemistry, some Quartz Crystal Microbalance (QCM) crystal uses silica quartz directly. Such crystals are readily available to be aptamer functionalized, which enables QCM to make selective detection of target molecules.

Chapter 3: Design of the system

The final design consisted of using covalent linkers to functionalize surfaces. The covalent immobilization of aptamers follows from the silane chemistry previously reported [7][26]. Because of the stability of the 2H phase TMDs (or other stable surfaces) and the corresponding

difficulty of functionalizing, an ALD layer of SiO_2 was warranted. Aside from being the easier functionalizing material, SiO_2 may also act as a protection layer for the surface underneath by preventing interaction with the analyte solution.

3.1 Silane Chemistry and Covalent Linkers

The silane chemistry behind the covalent functionalization is outlined in Figure 2 Scheme 1 [7]. The surface hydroxyl groups on the SiO_2 layers are reacted with (glycidoxypropyl)trimethoxy silane (GOPS) in Hydrochloric acid (HCl) aqueous solution (pH 3.5) for 4 hours with occasional shaking and constant heating in a sand bath at 90℃. The acid environment opens the epoxide ring on the GOPS and produces diol groups. Though other papers describe using GOPS to couple amine-functionalized aptamers to glass, Potyrailo et al. describe the epoxide ring in GOPS to be too reactive and has many bonding affinities to non-target amine-functionalized aptamers [7]. The diols which are now covalently bonded to the TMD (or other surface or native silica quartz) via the SiO_2 functionalization, are then reacted with carbonyldiimidazole (CDI) in acetonitrile (ACN) solution. The CDI creates a more amine-targeted binding site and prevents the nonspecific bindings associated with GOPS. The amine-modified aptamers in a Phosphate Buffered Saline (PBS, pH 7.4) buffer are coupled with the CDI moieties when micropipette the aptamer solutions into the barely substrate-submersed PBS buffer. Unreacted aptamers are rinsed away by PBS and dried in the air. To block unreacted surfaces, the substrate is incubated with 0.1 M ethanolamine solutions (brought to pH 9 with HCl) at 20℃ for 2 hours [7]. Blocking the unreacted surfaces was not attempted since the ethanolamine solution is quite hazardous; therefore, some sites on the sensing layer may be vulnerable to physisorbed material (buffer, aptamers, or other target molecules). Such a surface may change the mass readings of acoustic wave sensors, or the optical properties for an optical aptamer-based sensor, for every subsequent reuse of the device.

For sensing surfaces without silanol bonds, the surface of the material can be coated with silica from ALD as shown in Figure 2 Scheme 1. Since TMD surfaces grown by CVD are usually quite small in area, we would only need ALD on sections of the substrate with TMD keeping the rest of the substrate clean for probing measurement. One would have to look at the shape of the TMD under a microscope and build a mask of the shape of the TMD. Using the mask, one could ALD directly or spin positive photoresist all over the TMD surface. Then using the mask, expose the sections with TMD and bring the whole substrate to ALD. After silica deposition, one can etch away the remaining photoresists, which would also remove the silica directly above the photoresists. This masking method would ensure that there is only ALD silica on the TMD sites.

If the surface already has silanol bonds, the silane chemistry between the linkers to the surface can be applied directly as shown in Figure 2 Scheme 2. Defect generation via an oxygen plasma onto silica surfaces will create more hydroxyl bonds and may enhance the coverage of active bonding sites for linkers to react with.

Scheme 1: ALD Silica onto highly stable or Silanol-bare Surfaces

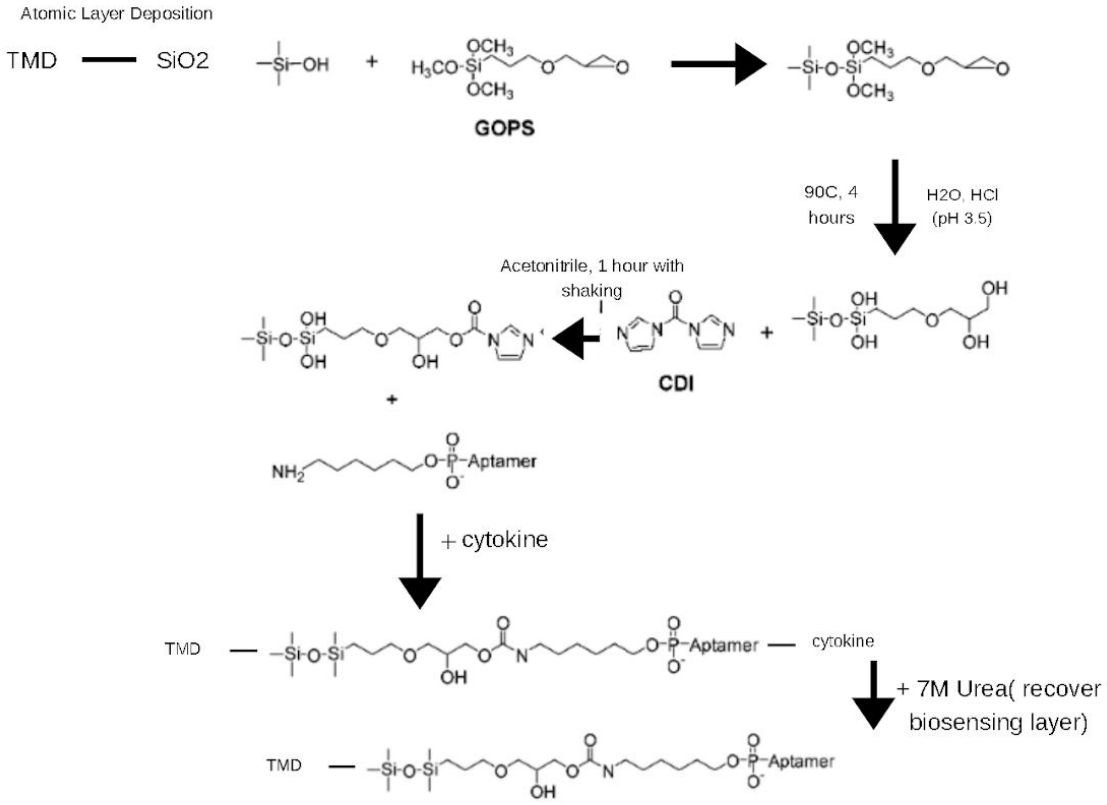

Scheme 2: Silica Surfaces (QCM quartz crystals)

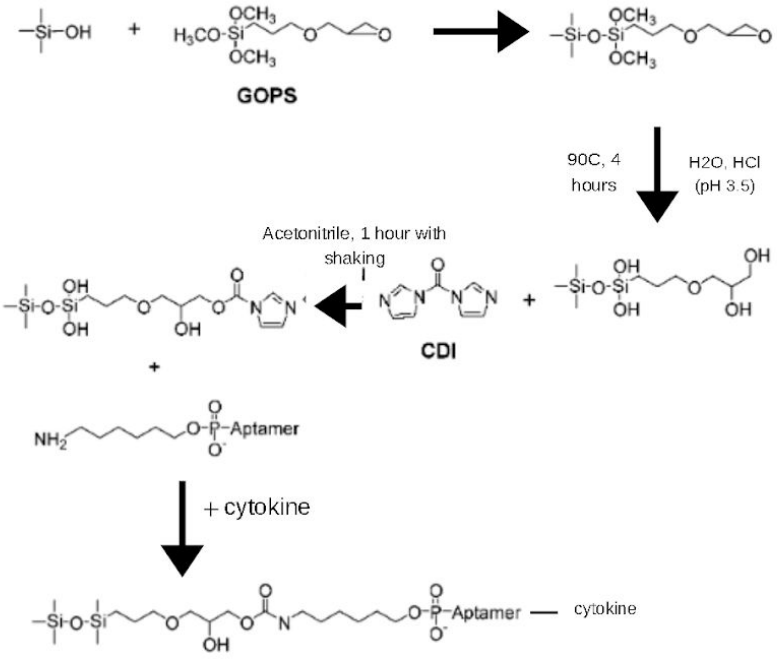

Figure 2: Covalent Immobilization of Aptamer. Modification scheme from [15, Fig. 3, 20, Scheme 2, Scheme 3, 21, Fig. 2]. Scheme 1 depicts the functionalization steps for silane chemistry via

ALD on surfaces without silanol bonds. Scheme 2 shows the fabrication process for surfaces with silanol bonds. Surfaces with silanol can be covalently attached to amine-terminated aptamers via the covalent linkers: GOPS and CDI. GOPS is attached to a silica surface by heating the substrate in a vial containing GOPS and acidic aqueous (pH 3.5) for 4 hours. The CDI is attached by soaking the substrate in an acetonitrile solution containing CDI and shook for 1 hour at room temperature. CDI-functionalized substrate is then soaked in a PBS solution containing amine-terminated aptamers overnight. This aptamer-functionalized substrate can then be reacted with cytokine and reused by rinsing off the cytokine with urea.

3.2 Hairpin Structure of Aptamer for Fluorescence Biosensing

Some aptamers bend back inwards when a target molecule (cytokine) is introduced. However, for the other aptamers that bend outwards, we would need to introduce a complementary chain to induce a light-emission difference. A hairpin structure of the aptamer, in which the end of the cytokine-targeting chain is modified with a section of complementary chain, will loop the fluorescent dye molecule back to interact with the TMD layer (dye quencher) or fluorescent dye quencher [5][15][16]. This looping back of the fluorescent dye molecule to be close to the quencher will enable the fluorescent molecule to be quenched, yet the aptamers do not leave the TMD layer because of the covalent bonds as shown in Figure 3. The immobilized aptamers will allow for subsequent sensing capabilities when the target cytokines are washed away with urea.

The current fluorescent aptamer biosensor tested does not have an innate quencher, like the TMDs'. To visualize the light emission change from fluorescent dye molecules' positional variations, one would induce the bending back of the aptamer with its complementary chain. When dye molecules are bent inwards, close to the surface, the light emission dims. On the other hand, the aptamer chains that bend outward, due to bounded target, would emit more light as shown in Figure 3.

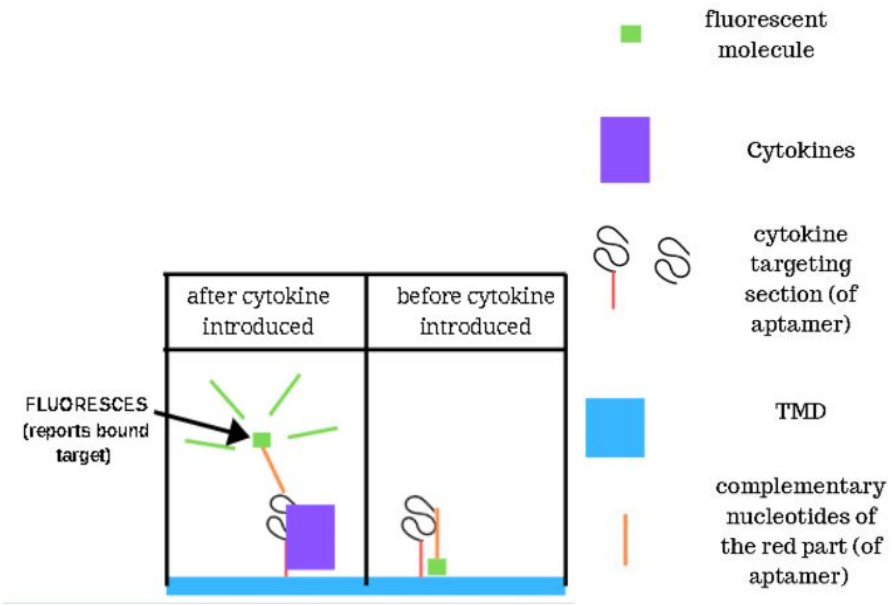

Figure 3: Optical Reporting Mechanism Details. Before cytokines are introduced, the aptamer loops inwards, bringing the dye close to the surface, because of the bonds with its complementary nucleotides. This inward bending results in a dimmer emission. When cytokines are introduced, the aptamer-complementary nucleotides' binding site is outcompeted by the aptamer-cytokine interaction. The bounded cytokine causes aptamer deformation resulting in the fluorescence dye moving to a new positional location: causing a brighter emission.

3.3 Reusability: Introducing and Dissociating Cytokine

The cytokines are introduced by diluting aliquoted contents in PBS to the required concentration and introduced by micropipette or syringe to the QCM O-ring where the functionalized silica substrate resides. One of the main purposes of this covalent bond design is for a multi-use device, so it would be important to release the cytokine samples post detection. A major benefit of aptamers over antibodies is aptamers' robustness in harsh conditions and its reusability; placing the whole functionalized layer in harsher conditions to remove the attached cytokines would not hinder the functionalized sensing layer's subsequent sensing capabilities. Some papers rinse the cytokines off by simply water or just PBS buffer solution. Potyrailo et al. rinse their glass slides with PBS followed by guanidinium hydrochloride, a high concentration (6 M) solution, which disrupted the ordered structure of proteins and then pre-equilibrated their device with PBS [7]. Urea is also a common solvent that is used to break the tertiary structure of proteins by destabilizing the hydrogen bonds. Some utilize 6 to 8 M of urea to rinse off the cytokines [5]. To remove the cytokines, 7 M urea concentration was used to break off the cytokine-aptamer bonds. One method worth exploring is whether heating with electricity or an incubator would dissociate the bonds between targets (cytokine) to the aptamers. Because the bonds between the target (cytokine) and the aptamer are much weaker than that of the covalent bonds existing between the silica surface and the aptamer, urea washing can remove merely the cytokine and reuse the biosensor. Such is comparable to boiling water breaks the hydrogen

bonds between water molecules but doesn't break the covalent bonds between hydrogen to the oxygen. Coincidentally, the composition of aptamers and single-stranded DNAs are the same and the main bonds holding double-stranded DNA together are hydrogen bonds.

Chapter 4: Experiment and Characterization

After every functionalization, it is ideal to get a direct characterization of the new chemical bonds formed. Material characterization ensures that the expected reactions have proceeded and the linkers are properly functionalized on the sensing surface. Common surface chemistry direct characterization uses Fourier-transform infrared spectroscopy (FTIR), Raman spectroscopy, and Ultraviolet-visible spectroscopy (UV-Vis). However, the characterization results were not as originally anticipated and did not show any discernible difference or expected bond characterization features between before-functionalization and after-functionalization substrate. Though most suitable for surface chemistry characterization, X-ray photoelectron spectroscopy (XPS) was forgoed due to the COVID-19 lab closure and preparation time for each sample. The intent is to do XPS characterization after the indirect characterization experiments are more stable and lab access resumes.

For this thesis, the surface material indirect characterization done were Thermogravimetric analysis (TGA), and mass-based and fluorescence measurement. For the mass-based measurements, QCM crystals were functionalized, and then the change in frequency induced by the added material (aptamer, buffer, cytokine, and urea) measured. All measurements were done in Phosphate buffered saline (PBS) for standardization purposes and eliminated the need to use Kanazawa and Gordon equation [28]. Optical emission is a lower intensity when Tumour Necrosis Factor-alpha (TNFa) is bound to the aptamer-functionalized surfaces because of the folding back of the fluorescence molecule. These characterizations are indirect because the exact bonds or material on the sensing layer are inferred based on other measurements (mass or optical changes).

A downside to indirect characterization is that linker bonds are unknown and can only be inferred based on the difference between the GOPS-CDI-functionalized surface and the added molecule mass or optical response difference (aptamer or target cytokines). To compensate, 7M urea washing was needed to check if the sensing layer is still recoverable and reusable for subsequent detecting. If the device was reusable, the linkers can be inferred to be covalently attached to the substrate surface; otherwise, the aptamers would have been rinsed off by the highly concentrated urea. In addition, selectivity tests were important to ensure optical or mass changes are caused by target molecules (cytokine) and not merely any random molecule. One can evaluate the selectivity of the sensor by testing the response against other non-target proteins: BSA, other types of cytokine, test aptamers...etc.

4.1 Characterization Results

Characterizing after every step, visualizing or quantifying aptamers on silica substrate are important to ensure the functionalization was successful. If the aptamers drop-casted onto silica substrate cannot be detected by the characterization machines, then surface-functionalized aptamers, of much lower concentration, will also not be detectable.

4.1.1 Raman

Raman spectroscopy measures the relative frequencies a sample scatters radiation [29]. These specific relative frequencies are characteristics of different bonds and can fingerprint the polarizing bonds present on the functionalized layer [29]. A pre/post functionalization comparison can present evidence of functionalization. Raman spectroscopy of GOPS functionalized silica surfaces is shown in the following figures. Bare silica gives off a peak at around 520 cm^{-1}. The following figures show the camera image of the region around the laser excitation area. Immediately after the sample microscope camera image of the GOPS-functionalized silica, the corresponding Raman measurement is shown in comparison to a blank silica substrate. Raw spectra taken from Raman are in Appendix A.

Figure 4: Raman Machine's Camera Image of the GOPS Functionalized Silica.

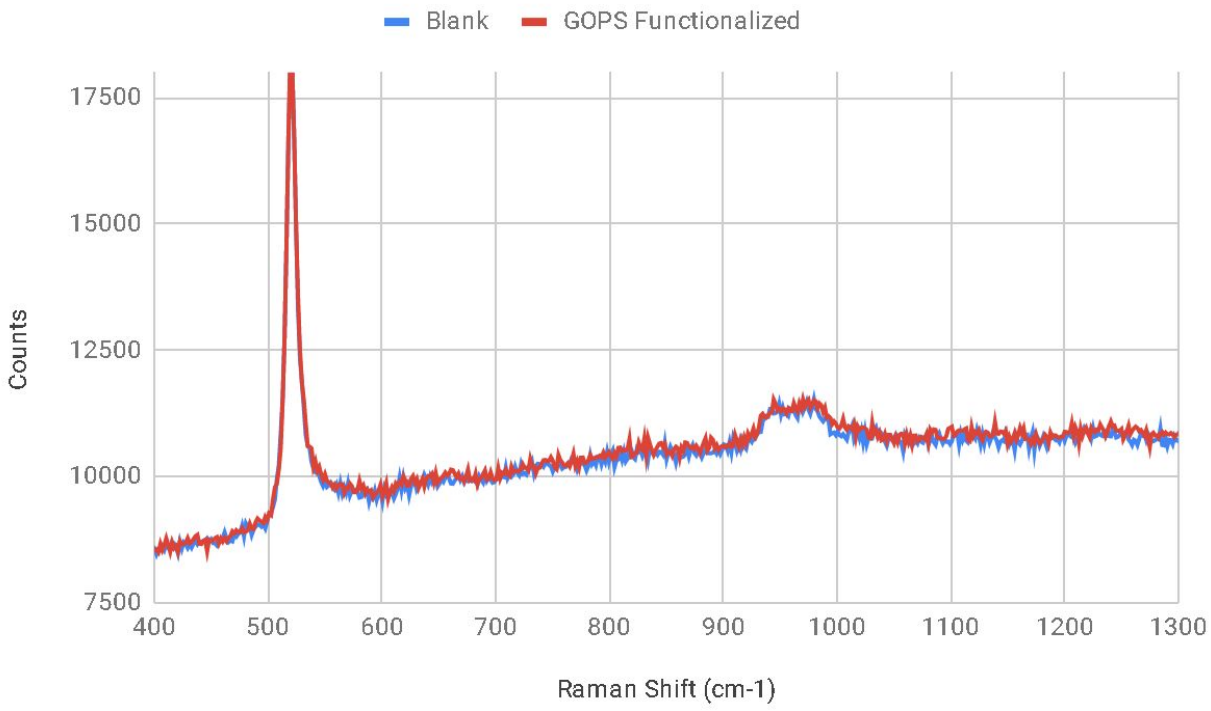

Figure 4.1: Normalized Raman Spectrum Comparison of the GOPS Functionalized Silica and Blank Silica. The results from taking multiple Raman measurements show no discernible difference between the Raman spectra of the non-purple coloured and the background purple regions.

Raman spectrums of functionalized silica showed no discerning peaks corresponding to the added GOPS material. There are only the distinguishable blank silica spectra: 520 cm^{-1} peak of blank silica and the less prominent 970 cm^{-1} peaks for silanol bonds. Raman spectroscopy did not support the presence of distinctive GOPS bonds, Carbon-Oxygen-Carbon, at the expected spectra location between 1180 and 1200 cm^{-1}.

4.1.2 Fourier Transform Infrared Spectroscopy (FTIR)

Complementary to Raman which detects changes in polarity, FTIR can be employed to see changes in dipole moment molecular bonds that are not evident from Raman [30]. Contrary to Raman, IR Spectroscopy measures the absolute frequencies at which the surface absorbs radiation [30]. FTIR (ATR, transmission, and reflectance mode) spectrums are usually complementary to Raman spectrums --- in that chemical bonds that don't show well in Raman usually have distinguishable peaks in FTIR.

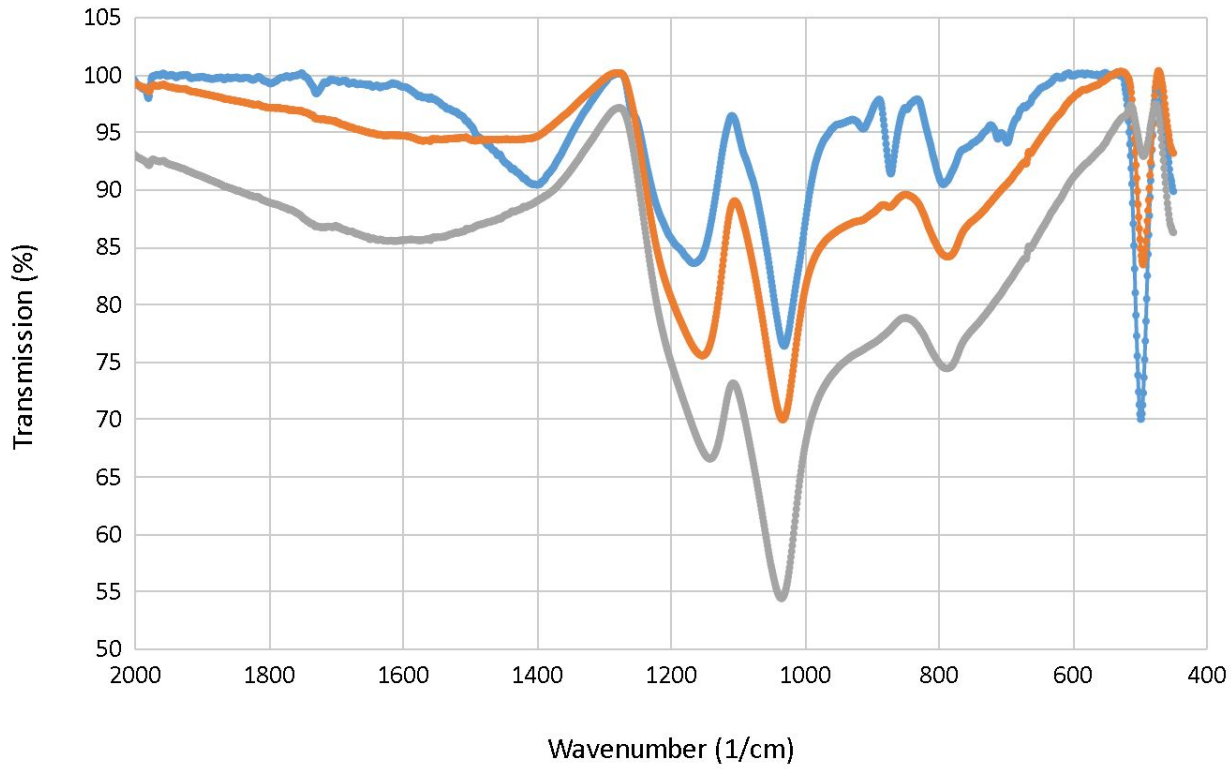

Figure 5: Normalized FTIR spectrum for Varying Functionalized Stages: Blank (Grey), Aptamer-functionalized (Blue), and Aptamer-functionalized interacted with Cytokine (Orange)

From the FTIR characterization results, there is no discernible difference between the FTIR peak positions for the aptamer functionalized silica and the blank silica. Likewise, no differences in spectra were observed for substrates exposed to cytokines compared to blank substrates. The peak at 520 cm^{-1} is part of the absorption typical of silica. This characterization did not detect any expected added material nor justify the presence of linkers.

4.1.3 Thermal Gravimetric Analysis (TGA)

Thermogravimetric analysis (TGA) is the process of heating a sample to 800℃ and measuring its respective weight loss. This method can be used to characterize surface composition based on weight loss when specific molecules reach their oxidation temperature. TGA in SFU's Chemistry Department is sensitive to a 10 ug weight difference. However, because the machine could only take 5 to 15 mg of material, the maximum (assuming 100% functionalization coverage) added weight from functionalized material was 0.1ug. The calculation is shown below in Table 1 [31-34]. The substrate area size is about 0.924 cm^2. Note cytokines were not added to the TGA sample to save on cytokine material and to test the TGA's sensitivity. Figure 6 is the TGA data acquired for the aptamer-functionalized silica substrate.

		Maximum # of			
Substrate area used in TGA	**Silanol [36]**	**GOPS**	**CDI**	**Aptamer**	**Cytokine**
cm^2	**$1/nm^2$**	**ng**	**ng**	**ng**	**ng**
0.1155	4.5	20.3	13.9	941.8	1510

Table 1: Estimation for the Max Coverage Weight of the TGA-sampled Substrate

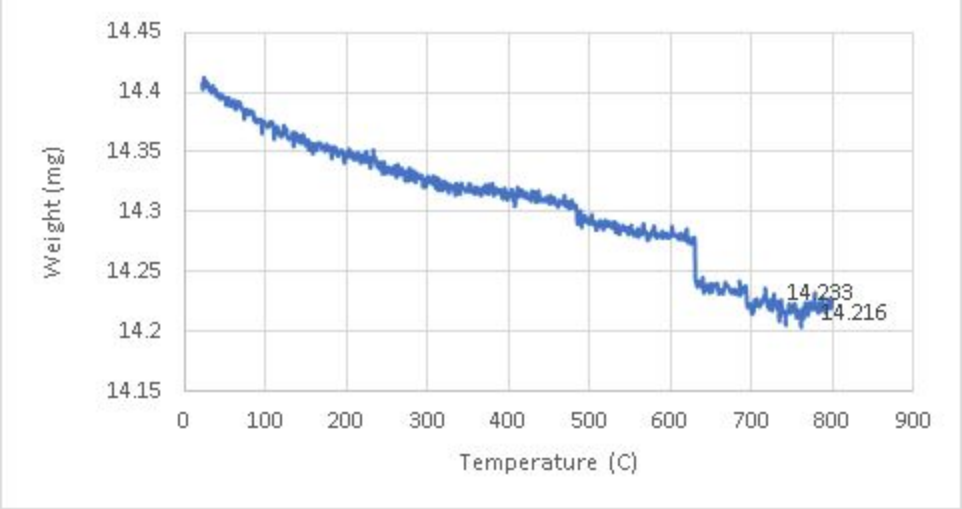

Figure 6: TGA Data for part of an aptamer-functionalized Silica

From the TGA results, the noise of approximately 0.02 mg from the machine is much greater than the described 10 ug. Needless to say, the 1 ug of the max weight of the added material (cytokine or aptamers) of the sensing layer would not be discernible from the TGA machine's sensitivity. In addition, this decrease in weight is also not expected: biological samples should be oxidized below 450℃.

4.1.4 Ultraviolet-visible Spectrophotometry (UV–Vis)

Tan et al. reported UV-Vis spectroscopy as a simple method for detecting the aptamer-functionalized gold nanoparticles [35]. Jing et al. describe aptamers to absorb wavelengths lower than 300 nm with maximum absorption at 260 nm, whereas proteins' absorption in the near UV range (250 - 300 nm) is "really weak due to aromatic residues" and comparable to aptamer in the far UV range (lesser than 250 nm) [36]. The difference in spectrum between plain deionized water and that of a solution with 10 ug of cytokine is shown in Figure 7. The spectra collected for deionized water and increasing dilution of 10 ug cytokine in DI water are shown in Figure 7.

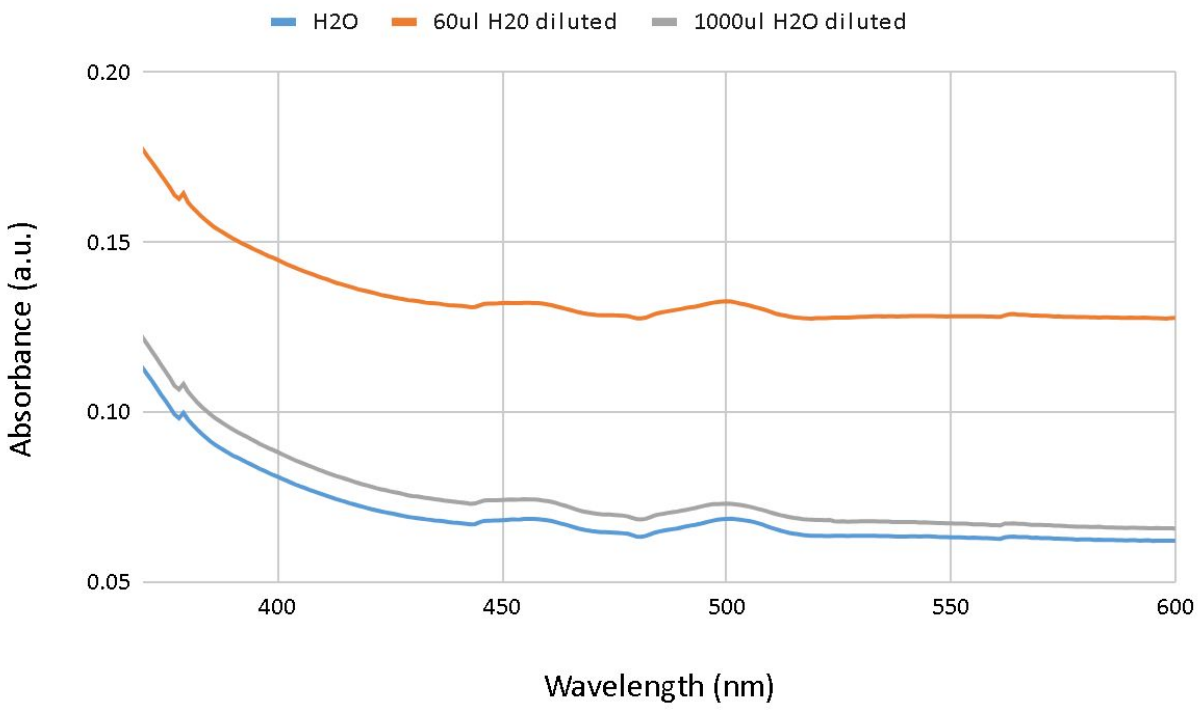

Figure 7: UV-Vis Spectrum of Varying Concentration of Water Diluted cytokine versus Plain Water

There is no discernible difference between the cytokine solution to that of a water solution. The deionized water spectra conform with Toshifumi Uchiyama's water analysis UV-Vis spectrum. This means that even if the surface is functionalized and interacted with the cytokine, UV-Vis would not be able to report the presence of the added cytokine. UV-Vis was also not informative to determine if my device was properly functionalized.

4.1.5 Fluorescence-labeled Aptamer (Optical Biosensing and Characterization)

By covalently attaching a fluorescent molecule to the aptamer end, the aptamer can be visualized via a fluorospectrometer with laser excitation. If the substrate has fluorescence after the aptamer functionalization step, then the functionalization was successful. Without covalent linkers, the fluorescence readings of just physisorbed aptamers on the substrate are much lower than that of the readings from a covalently linked substrate. Moreover, using this dye visualization technique, the washing-off step of physisorbed aptamers was established. As long as the aptamers did not dry on the substrate, to wash off the physisorbed aptamers in a PBS submersed substrate, the substrate was rinsed with PBS and water solution. On the other hand, when the aptamers are covalently attached to the substrate, multiple urea and PBS washing would not remove the aptamers and the substrate continued to fluoresce. Figure 10 shows the different orientations of aptamer dyes and the corresponding benefits or challenges to optical

sensing. Figure 10 Scheme 1 outlines the challenges to the random orientation of dyes, which may falsely indicate cytokine attachment. Figure 10 Scheme 2 describes a method to consistently align the fluorescent dyes' orientation: using the interaction of complementary chains to the cytokine-attaching aptamer nucleotides. Figure 10 Scheme 3 is a hypothesized method that uses built-in quenchers and dyes to make any aptamer-functionalized surface become an optical biosensor.

Based on Förster resonance energy transfer (FRET), if the fluorescent molecule is far from the quencher, the fluorescent signal should be emitted. Because TMD is a highly efficient fluorescence quencher (up to 97% quenching), if the fluorescent molecule is moved away from TMD, then the fluorescent signal should be resumed. The tertiary structure of aptamers changes when in contact with targets, which induces a FRET signal. Figure 10 Scheme 1 illustrates this effect. When the aptamer is in the solution with the target cytokine, the fluorescence signal will be unquenched because the quencher will have a lower affinity to the aptamer than that of the target cytokine-aptamer bond as shown in Scheme 3 of Figure 10 [37]. In Scheme 3, the quencher is forced to move away from the dye; therefore, induces a fluorescence change.

The aptamer-captured cytokines induce a charge transfer and change the fluorescent signal. The fluorescence change can be used as a biosensing indicator of the captured target fluorescence signal. Because the orientation of the fluorescent dye is not always limited to the TMD surface, as shown in Figure 10 Scheme 1A, that specific aptamer will be fluorescing even prior to the attachment of the cytokines. If the cytokines do not induce a different fluorescent signal, then that specific probe will not give useful indications of cytokine presence.

To avoid random-orientation induced false positive signal, complementary nucleotides are appended to the cytokine-capturing aptamer nucleotides as shown in Figure 10 Scheme 2. In the absence of the higher bind-affinity cytokines, the appended complementary nucleotides would bend inwards to create hydrogen-bonds with the original aptamer nucleotides. The inward-bending dye orientation would consistently, unlike the randomness in Figure 10 Scheme 1, create a dimmer fluorescence intensity prior to interacting with the outward bend-inducing cytokines. Contrary, for aptamers that bend inward when cytokines attached, the complementary chains would bend at the aptamer-end further from the surface. From this complementary-characterization configuration, a target-bounded reporting mechanism is also achieved.

If the biosensing base surface layer is not a dye quencher, like the TMDs, a quencher can be built into the middle chain of the aptamer sequence and the complementary chain would simply hairpin loop back to the quencher as shown in Figure 10 Scheme 3. Despite the possibility of a more drastic difference in fluorescence intensity, the built-in quencher in the aptamer sequence will carry the downside of the additional associated cost.

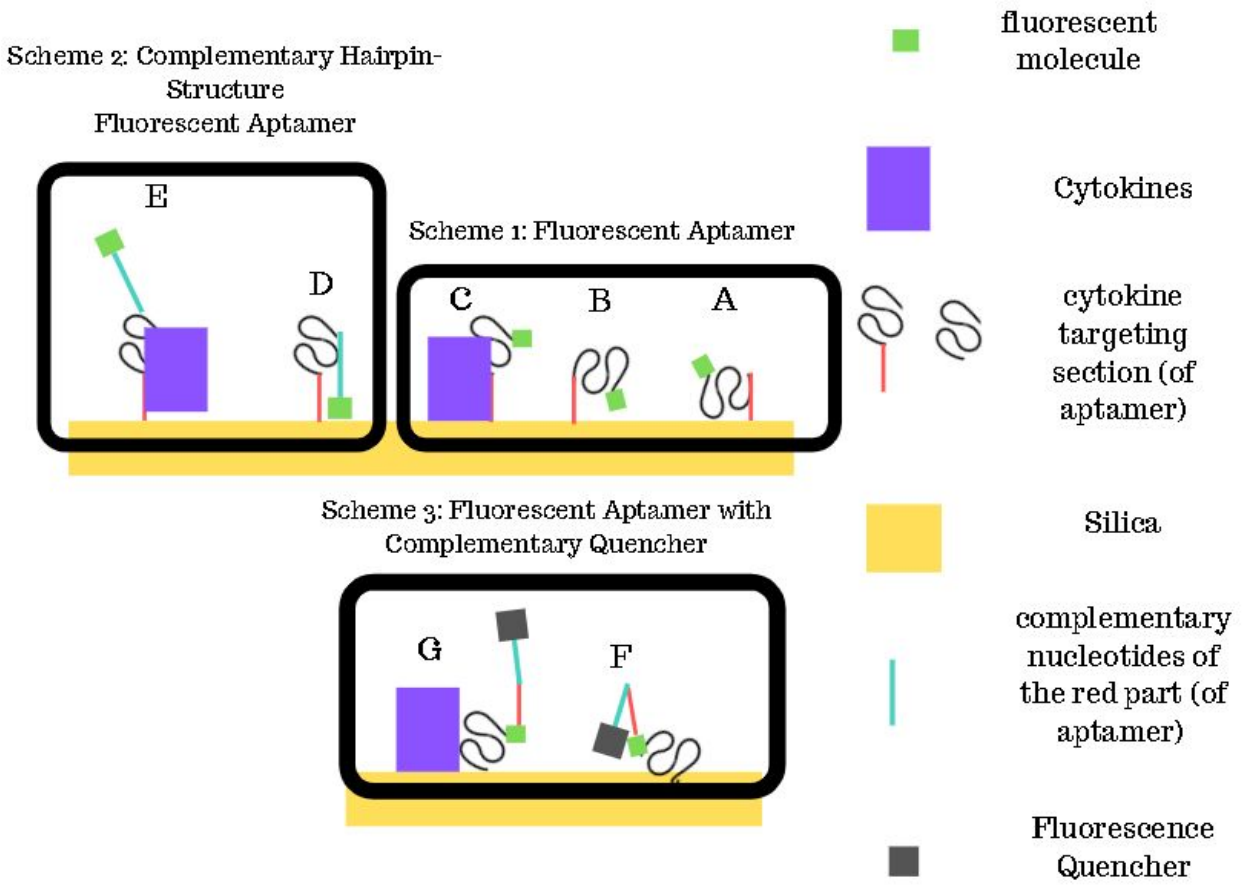

Figure 10: Different Methods of Fluorescent Biosensing

The following are the optical characterization and optical sensing results. These characterizations could only happen after GOPS and CDI functionalization steps because the fluorescent dye molecule is only built into the aptamer sequence. Figure 11.1 shows the excitation location. Note the excitation laser is normalized every day to the excitation wavelength of 480 nm before measurement. Figure 11.2 is the bottom middle portion of a functionalized silica's fluorescence spectra. Figure 12 shows the fluorescent spectra of the bottom right portion of a functionalized silica substrate.

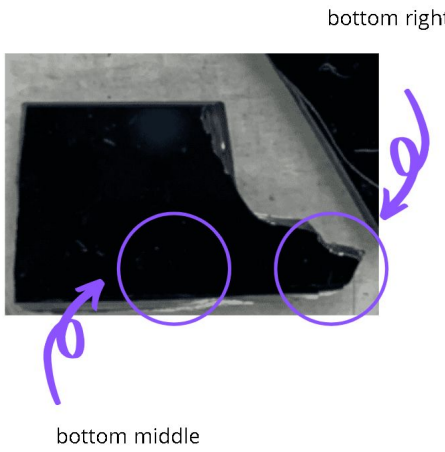

Figure 11.1: Excitation Location on the Aptamer-functionalized Silica

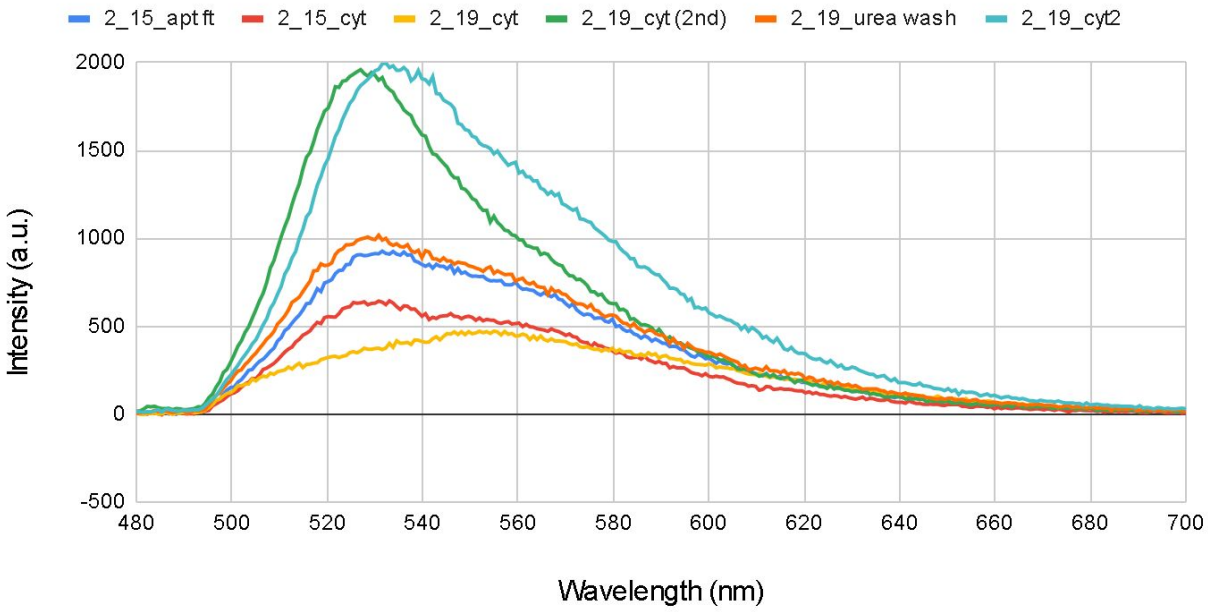

Figure 11.2: Fluorescence Spectra of Covalently-functionalized Silica (bottom middle portion)

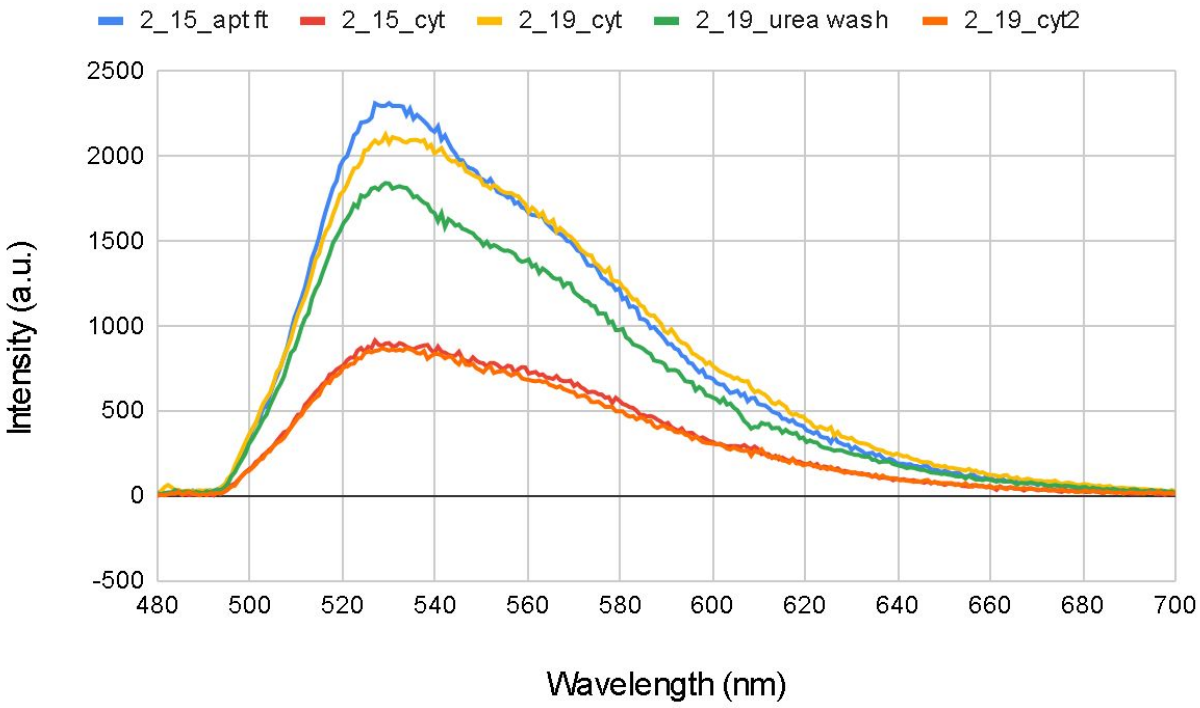

Figure 12: Fluorescence Spectra of Covalently-functionalized Silica (bottom right edge)

Notice that sometimes the cytokines do not induce a change in fluorescence and show the same intensity as the aptamer-functionalized or after urea rinse. The lack of change in fluorescence intensity demonstrates inconsistency in the biosensor optical sensitivity. This may be due to the smaller laser spot size compared to the overall substrate area (factor of 1/20), which cannot give a global functionalization picture of the overall device. Because of sterics or other structural limitations, not all the aptamers will be able to capture cytokines every time.

Figure 11 shows a bright fluorescence emission at about 2000 a.u., this immediately dropped to about 500 a.u. when cytokines are introduced. This means that the aptamers are changing shape to conform with the higher affinity cytokines' binding. Once the cytokines are rinsed off with 7M Urea, the fluorescence intensity recovered back to about 1000 a.u.; this is not the original aptamer intensity which may be due to random positioning of the aptamers or remaining cytokines as described in Figure 10's Scheme 1. However, upon more flushing with PBS (introduced when introducing the second interaction of cytokine), the original cytokines seem to be removed or the aptamers are back to original positioning (evident in the same original intensity as the aptamers'). In the second introduction of cytokines, they did not induce fluorescence changes, which is probably due to poor binding with cytokine or that the device was not reusable. But based on Figure 12's results, I think the lack of fluorescence change is due to the region not binding with cytokine simply because the incident light area is too small.

Figure 12's urea wash did not change the fluorescence intensity, which means that there was no cytokine interaction the first time. This means that the small region I am doing fluorescence measurements on will not always capture cytokines --- Figure 12 showed cytokine detected after the urea wash but did not for the first cytokine interaction. To avoid this limitation and obtain a

more global picture of captured material using optical aptamer-based sensing, I would need to get a larger, more uniform incident light intensity profile. Otherwise, this fluorescent measurement can only be used as a characterization to see if aptamers are functionalized on the silica.

Taken from SFU's MBB department's Chemidoc spectrometer machine, Figures 13 and 15 show images from functionalized-silica, SiO2-TMD substrates as a function of each step in the sensing. After image thresholding (segmentation technique based on pixel intensity) on the substrates, the corresponding bottom four images are displayed in Figure 13. Note that this set of functionalization is for a different kind of cytokine: Interferon Gamma (IFN). Upon attachment of cytokine (IFNg) to the aptamer, the substrate will get brighter because the fluorescent dye is moving outwards from the sensing surface. Figure 14's data was captured from SFU's Nanodevice and Fabrication Group's photo spectrometer showing the intensity difference between before and after cytokine interaction.

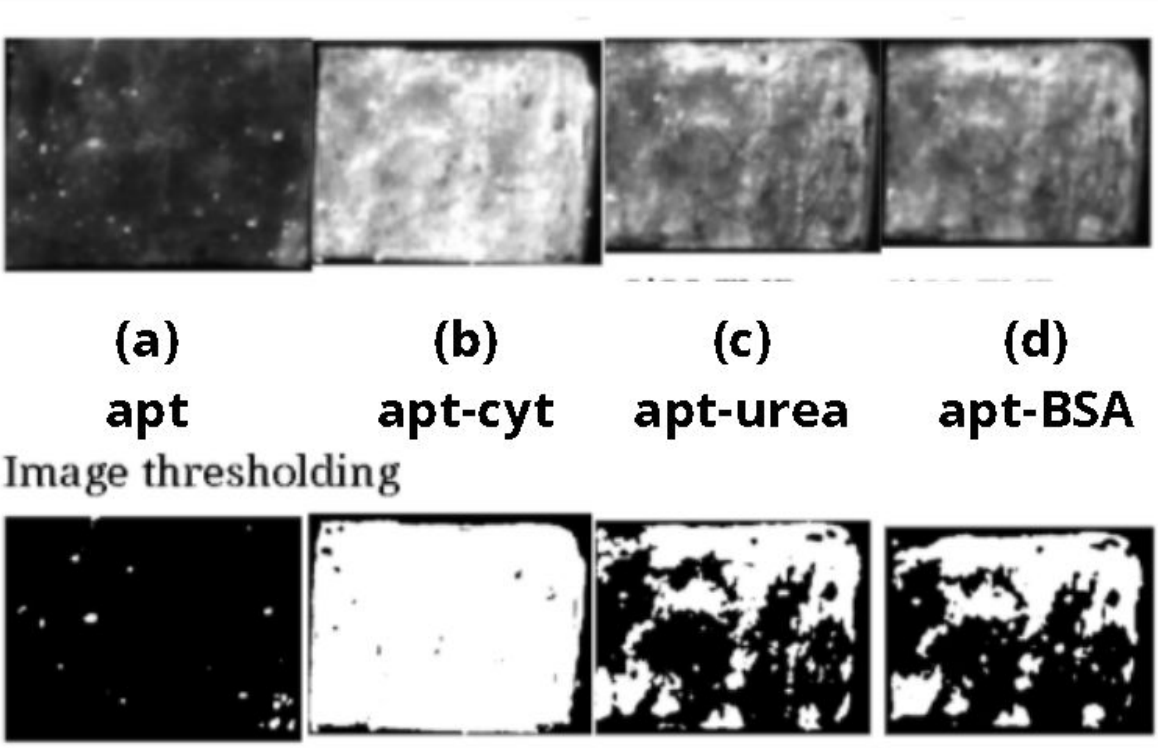

Figure 13: Functionalized Silica Substrates for Interferon Gamma (IFNg) Cytokines. (a) shows the fluorescence signal with aptamer functionalized (b) shows the fluorescence signal with IFNg reacted with aptamer (c) shows the dimming of the substrate after rinsing the surface with urea (d) shows not much fluorescence intensity change with BSA reaction with the sensing surface. Corresponding Otsu image, pixel value intensity threshold are displayed underneath.

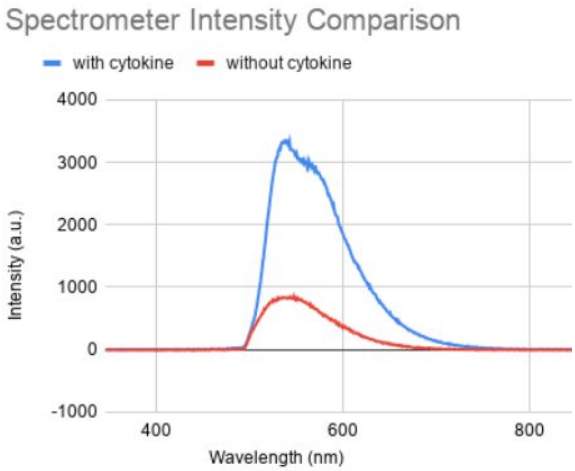

Figure 14: Functionalized Silica with Interferon Gamma (IFN) Aptamers and interacted with IFN Cytokines' Fluorescence Spectrometer

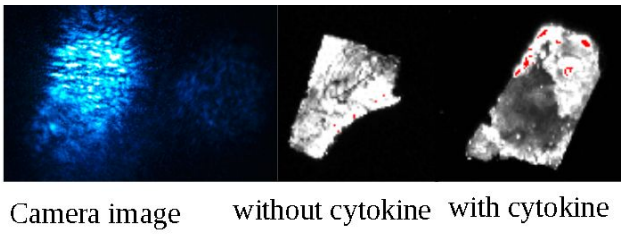

Figure 15: Functionalized Silica with Interferon Gamma (IFN) Aptamers and interacted with IFN Cytokines Camera and Chemidoc Spectrometer Images

As evident in Figure 13 and Figure 14, there is a clear brighter substrate after cytokine interaction, reduced brightness from urea wash, and relatively the same brightness when a non-target molecule, Bovine Serum Albumin (BSA), was introduced. The fluorescence signal only shows a noticeable difference when the target, IFNg, introduced as compared between Figure 13 (a) and (b). Furthermore, very little change in fluorescence signal is observed between Figure 13 (c) to (d) showing the specificity of the aptamer-based sensing layer. The areas in red in Figure 15 indicate saturation of the photodetectors.

4.1.6 Quartz Crystal Microbalance (Mass-based Biosensing and Characterization)

Quartz Crystal Microbalance (QCM) is able to determine the resonant frequency of the quartz crystal [2][28][38-40]. When the quartz crystal is functionalized with the material, the weight would increase and the corresponding resonant frequency of the crystal would decrease. Equation 1 and Table 2 outlines the relation between change in frequency to change in mass [28][38-42]. Because all measurements were carried out in PBS buffer, the Kanazawa constant was not included [38][41].

$$\Delta f = -2f_0^2 \Delta m / (A\sqrt{\varrho_q \mu_q}) \quad \text{(Equation 1)}$$

F_0 (resonant frequency in buffer)	Pq (quartz density)	Uq (shear modulus)	A (area of quartz silica)	Change in freq	Change in mass
Hz	**g/cm^3**	**g/cm s^2**	**cm^2**	**Hz**	**g**
10005475 (taken from Figure 3)	2.648	2.947x10^{11}	0.924 (60% silica)	Depends on measurement	Calculated value

Table 2: Constant values for the Sauerbrey Equation

The following are the QCM measured changes in frequency data. Each figure represents a different stage in functionalization from Silica-GOPS-CDI functionalized, Silica-GOPS-CDI-aptamer functionalized, Silica-GOPS-CDI-aptamer-cytokine functionalized to 7M Urea rinse.

Figures 16 to 18 show results from QCM measurements. The odd resonant frequency spikes at the beginning of the experiment or the middle of the experiments are caused by the flow of PBS buffers or other solutions through the QCM channel into the O-ring. I had to wait for about 5 minutes for the system to equilibrate and reach a steady-state. The steady-state value in Figure 16(a) is the initial resonant frequency, f_0, used in Equation 1.

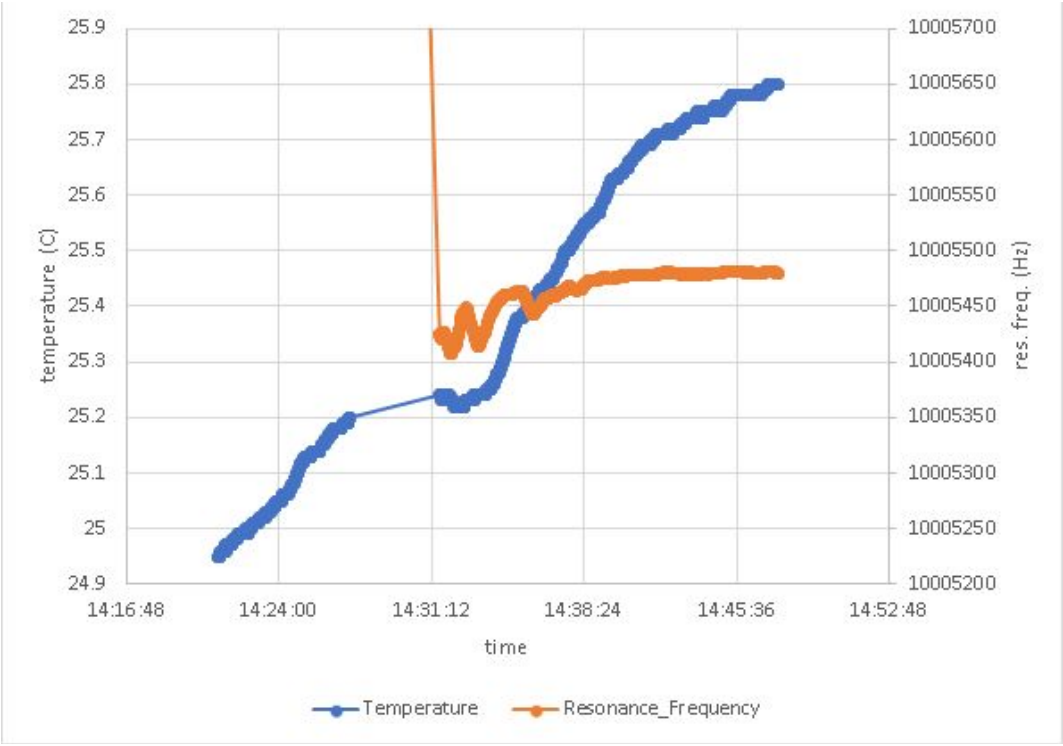
25.9
25.8
25.7
25.6
25.5
25.4
25.3
25.2
25.1
25
24.9
temperature (C)
10005700
10005650
10005600
10005550
10005500
10005450
10005400
10005350
10005300
10005250
10005200
res. freq. (Hz)
14:16:48
14:24:00
14:31:12
14:38:24
14:45:36
14:52:48
time
Temperature
Resonance_Frequency

(a)

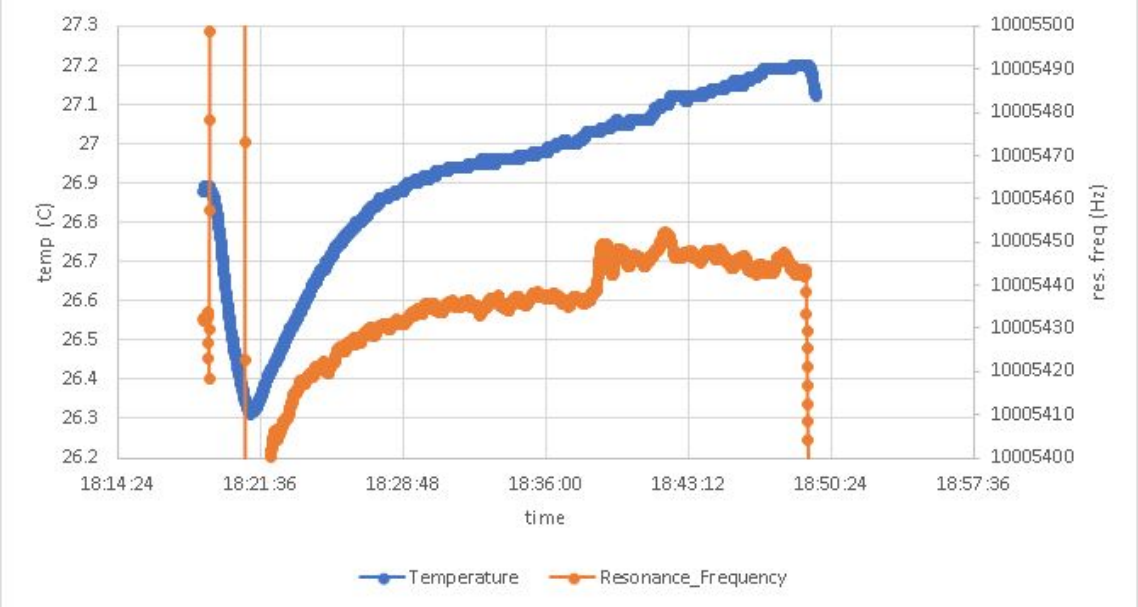
27.3
27.2
27.1
27
26.9
26.8
26.7
26.6
26.5
26.4
26.3
26.2
temp (C)
10005500
10005490
10005480
10005470
10005460
10005450
10005440
10005430
10005420
10005410
10005400
res. freq (Hz)
18:14:24
18:21:36
18:28:48
18:36:00
18:43:12
18:50:24
18:57:36
time
Temperature
Resonance_Frequency

(b)

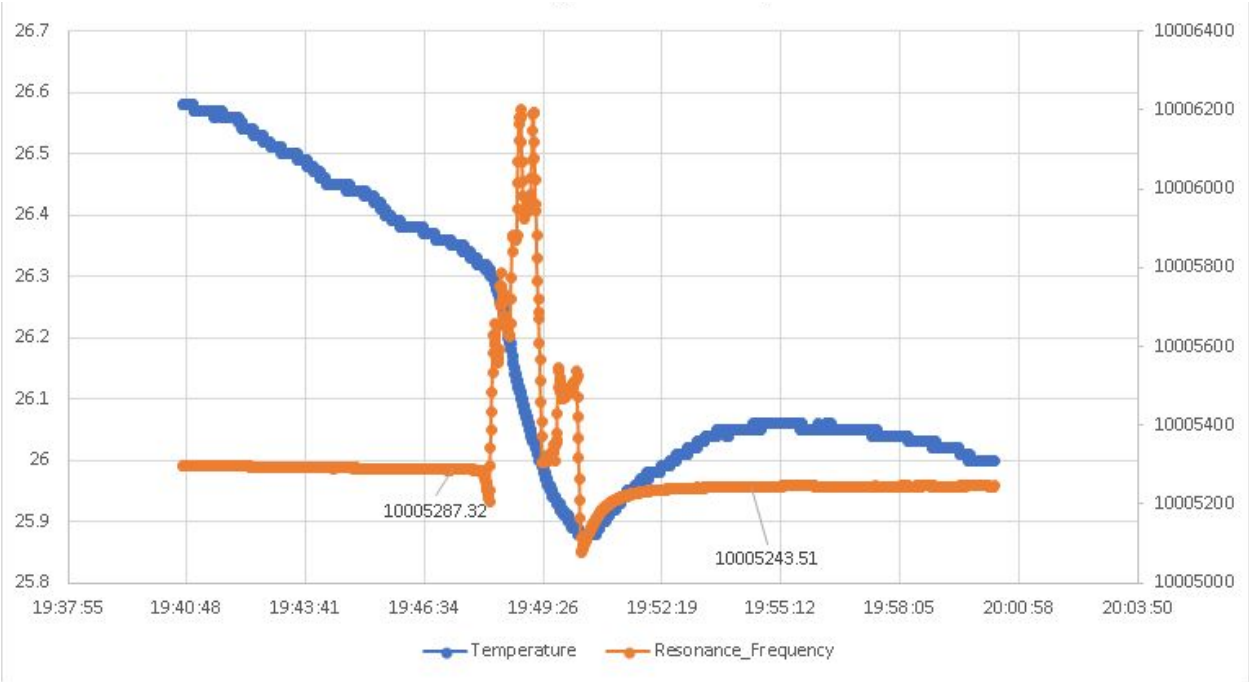

(c)

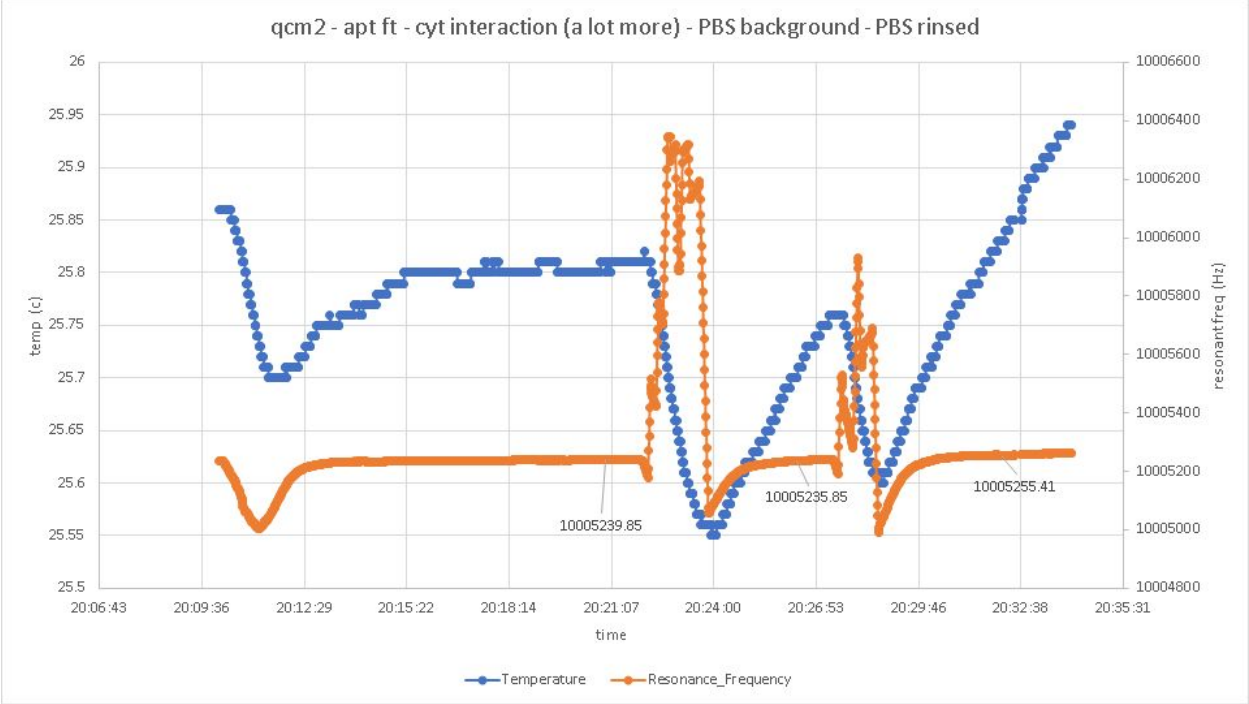

(d)

Figure 16: Temperature and Resonance Frequency as a Function of Time from QCM Measurements on (a) GOPS-CDI-functionalized (b) GOPS-CDI-aptamer (c) GOPS-CDI-aptamer-cytokine (d) GOPS-CDI-aptamer-cytokine (second cytokine interaction)

Figure 16 (c)'s pre spike peak is a steady-state value from the crystal in PBS buffer diluted cytokine solution. The spike is from washing off unbounded cytokine with PBS solution. Post spike steady-state values, measured in PBS, are the comparison values used between measurements.

This experiment in Figure 16 (d) is to test the limit of the QCM functionalized crystal's detection limit. The first peak fluctuation is from introducing a higher concentration of cytokine. The second peak fluctuation is from PBS rinsing out the unreacted cytokine. From this experiment, we could see the net steady-state frequency raised by 16 Hz. This means that some of the cytokines that are in the previous experiment, Figure 16 (c), are not bounded by the aptamers and are physisorbed. Because these cytokines are physisorbed, they are easily washed off by merely PBS rinsing. The cytokines that remained were probably the upper detection limit for this particular sensing layer: net 26 Hz (calculated from Figure 16 (c) and (d)).

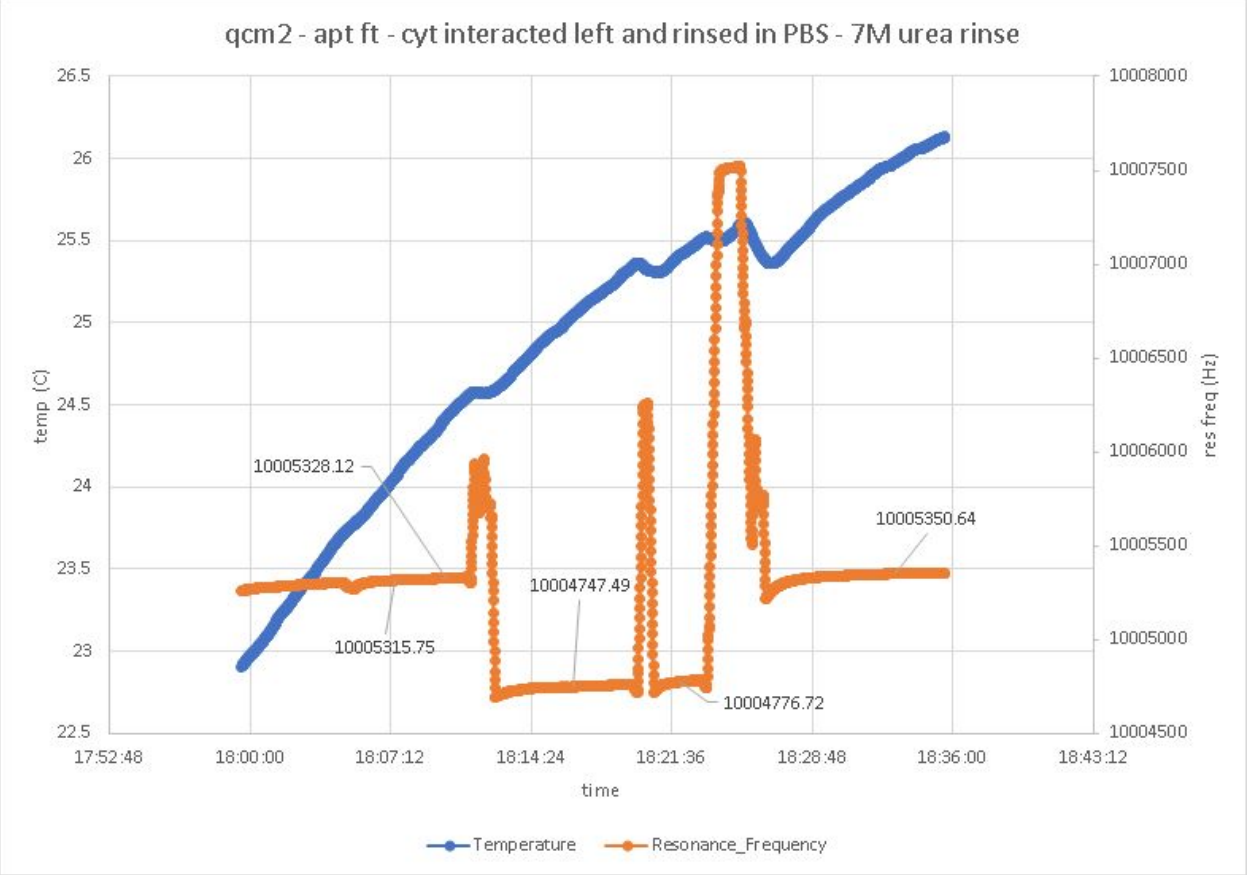

Figure 17: 7M Urea Washing Post-cytokine Interaction

The first peak fluctuation is due to the washing with 7M urea into the O-ring that has the cytokine interaction with the aptamer-functionalized substrate. Note the cytokine interacted substrate was left in PBS buffer overnight. The second peak fluctuation is another urea rinsing.

The last peak is from PBS rinsing. Notice the 22 Hz increase difference. This should signify that most of the cytokines have been removed.

4.1.7 X-ray Photoelectron Spectroscopy (XPS)

X-ray Photoelectron Spectroscopy (XPS) is a surface sensitive quantitative spectroscopy that works by detecting the number of electrons and its respective energy level. Such characteristic spectra readings correspond to a specific element and bond type. This characterization method has high sensitivity for surface chemistry and gives accurate percentage coverage information, which can compare with the estimation from QCM (20% aptamer coverage and 25% cytokine coverage; calculation is similar to TGA). I have not yet received data from this characterization method because of the COVID-19 lab closure. I will be doing this in the near future though.

4.2 Results and Discussion

From the optical and QCM's mass-based characterization data, the aptamers are being functionalized on the surface and are able to sustain a 7M urea wash. Therefore, the sensing layer is reusable for subsequent testing and most likely has covalent bonds.

4.2.1 Fluorescence Optical Biosensing

There is a significant difference between using covalent linkers and not using linkers. To compare, both types of substrates (blank silica substrates and functionalized-silica substrates) were submerged in PBS containing fluorescent-labeled aptamers for 1 day and rinsed with water after taking the substrates out. Under the excitation wavelength, a distinct fluorescence signal was observed in the substrate with covalent linkers. However, no discernible fluorescence emission was observed from the blank silica until at least 6 days of soaking. This comparison shows the difference between physioadsorbed aptamers compared to linker-induced functionalization.

The fluorescence dye method of reporting cytokine interaction is not always consistent because of the small light spot area. Sometimes the light spot would just by chance of sterics or physical configuration not be interacting with a cytokine. Regardless, current fluorescent dye configurations can still report aptamers' presence on the silica functionalized surface. The objective of characterizing the surface was achieved and moving forward with a mass-based detection method has the following benefits: reduced cost from not having to buy fluorescent dye-labeled aptamers and the extra complimentary chains' nucleotide sequence, and easier measuring techniques by eliminating the need to re-induce the complementary chain bonding after every urea wash and repositioning the substrate. With QCM, a global cytokine-induced response not limited to a section of the substrate area is possible.

4.2.2 QCM Mass-based Biosensing

A summary is shown in Figure 18 detailing the mass changes throughout the various stages of functionalization or cytokine interactions. The values are pretty reasonable where added weight corresponds to functionalization steps and decreasing weights corresponds to washing steps as outlined in Figure 18.

From the reusability experiment of using 7M Urea, the unaccounted mass (frequency) could be due to residue urea or cytokine on the substrate that did not get removed. Another possibility for the frequency discrepancy is probably due to the temperature fluctuations, which changes the resonant frequency readings slightly. To account for this, temperature data were collected alongside the resonant frequency data. Ideally, these temperature discrepancies can be accounted for.

The sensing layer is able to rid 84.6% of the bounded cytokine. This means 85% of the sensing layer can be reused to detect for more cytokines. The idea is that more of the sensing layer can be recovered with more urea rinsing.

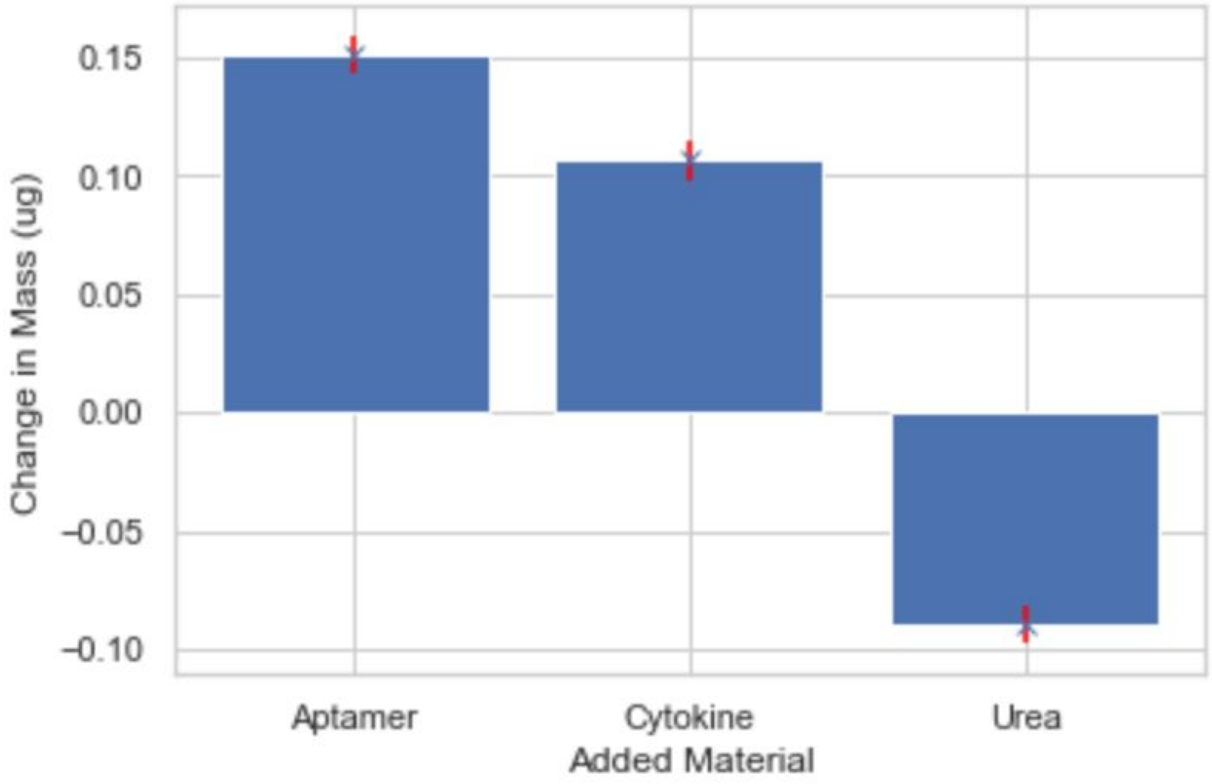

Figure 18: Summary of Mass Difference Corresponding to Various Functionalization Stage on QCM crystal #2

Figure 19 shows the difference in peak resonance frequency after adding target-cytokine, TNF alpha. There's a clear drop in resonance frequency by 60 Hz compared to the biosensing layer in PBS solution background.

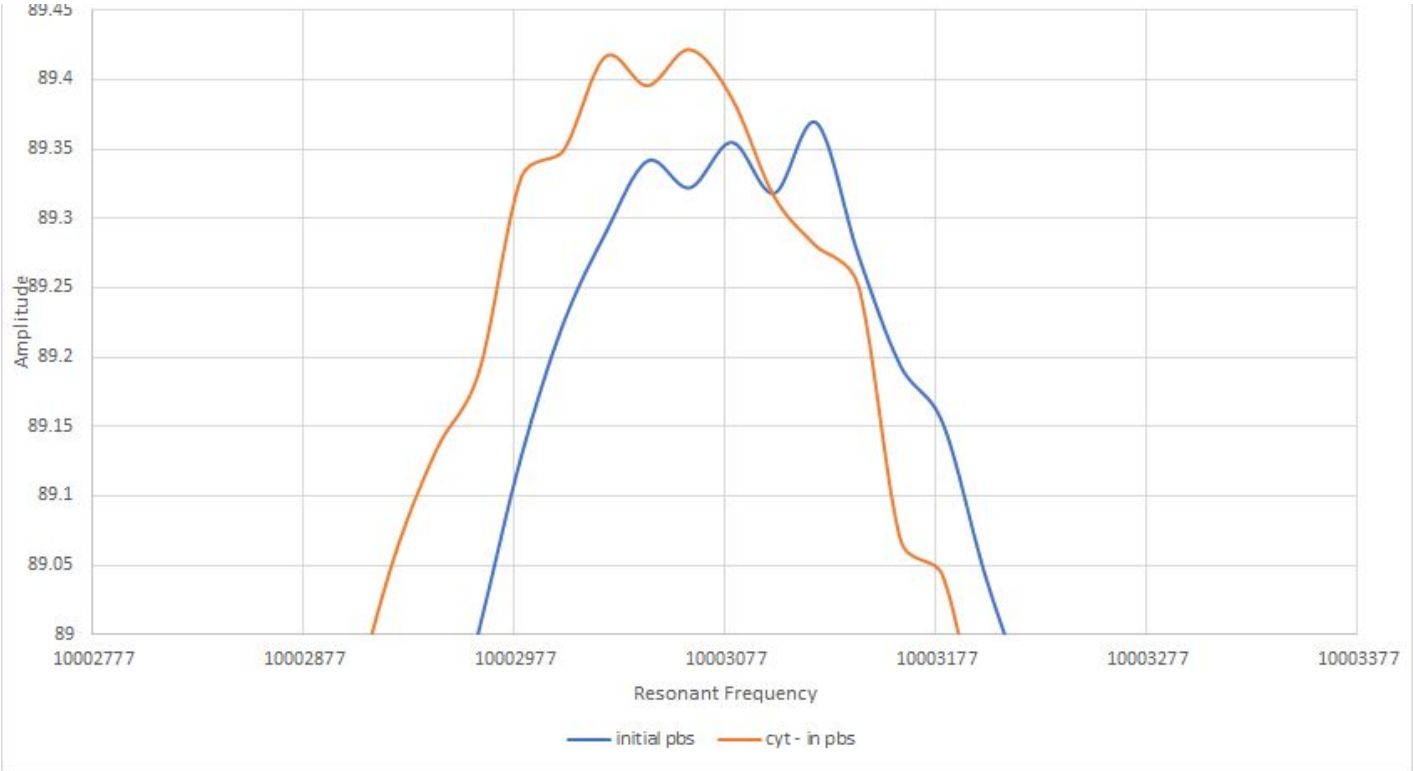

Figure 19: Comparison of Resonant Frequency after Cytokine interaction

The following results are from a second crystal, QCM crystal #3. Table 3 and Figure 20 show the result from QCM measurement showing the reusability and sensitivity of the biosensor to the target cytokine TNF alpha. Notice that the sensing layer is still active and able to be used for testing days after it's been functionalized and used. Note that between October 21 and October 22, the amount of recoverability of the surface is almost identical. On the first day, 32% of the surface was recovered for subsequent measurement via urea rinsing. The next day, the freed-up aptamers are then once again able to detect more cytokines ---- almost up to the maximum amount of cytokines that were removed the day before by the urea rinsing. Again, the urea washing removed 83% of the bounded cytokine on the second day. The third measurement was taken a week later, still showed the sensing layer able to detect the 1 ug of target cytokine.

	Added material	Change in resonant frequency
	ug	Hz
Oct 21	Cytokine (0.8 TNF Alpha)	-41
Oct 21	Urea rinse	+13
Oct 22	Cytokine (0.5 TNF Alpha)	-12
Oct 22	Urea rinse	+10
Oct 29	Cytokine (1 TNF Alpha)	-80

Table 3: Target Reusability Test Spanning Different Days

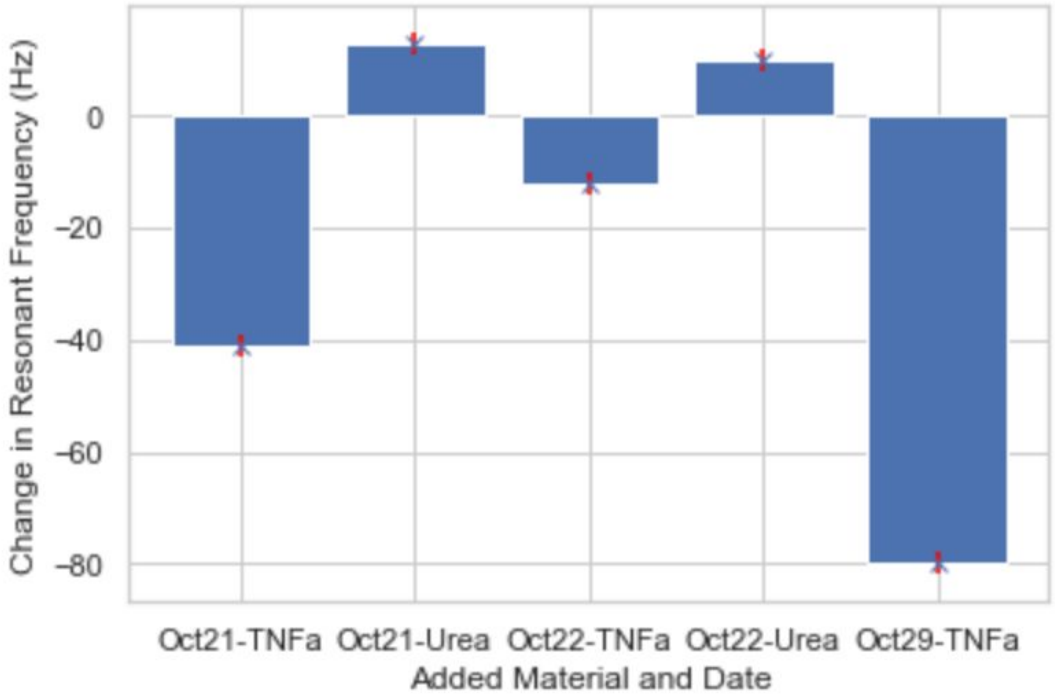

Figure 20: Target Reusability Test Spanning Different Days.

Table 4 and Figure 21 show the QCM results for the selectivity test of a non-target cytokine, Interferon-gamma (IFN Gamma). Notice that the amount of cytokine of IFN gamma type and the target cytokine, TNF alpha, that were used are the same. However, for the non-target cytokine, IFN gamma, the QCM does not elicit a response and there is no change in resonant frequency. Though a much smaller change in resonant frequency response than from 1 ug of target cytokines, it's noteworthy that at a much higher amount of 41 ug of non-target cytokine, IFN

gamma, the QCM does elicit a response. This means that the device could still be responsive to other non-target proteins, but would require a much larger amount than that of the target protein's amount. Interestingly, the amount of non-target proteins, IFN gamma, is able to be easily rinsed off with urea and the surface is 46% recoverable.

	Added material	**Change in resonant frequency**
	ug	**Hz**
Oct 23	Cytokine (1 IFN Gamma)	0
Oct 23	Cytokine (2 IFN Gamma)	-1
Oct 23	Cytokine (41 IFN Gamma)	-13
Oct 23	Urea	+6

Table 4: Selectivity Test with different amount of IFN Gamma Cytokine

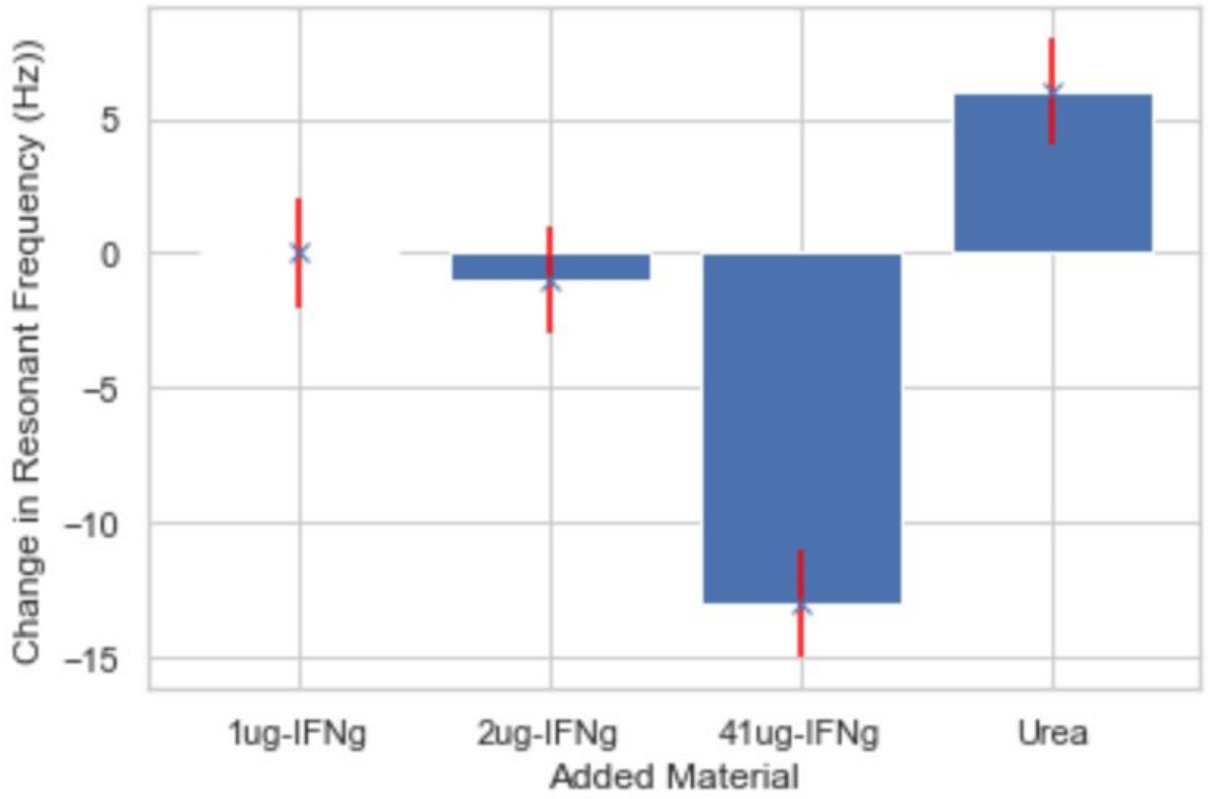

Figure 21: Selectivity Test with different amount of IFN Gamma Cytokine

Because both the cytokines tested before are in a solution that contains 50 ug Bovine Serum Albumin (BSA) to every 1 ug of cytokine, it's worth testing the effect from BSA on QCM measurements as shown in Table 5 and Figure 22. The BSA does not decrease the resonance

frequency of the QCM measurement, which means the BSA is not adding mass or sticking to the sensing layer. However, this result is not as conclusive because the crystal had previously been exposed to cytokines, which can interact with the carrier protein, BSA, to either stick or remove the cytokine. The removal of cytokine may be the reason for the increase in resonance frequency (decrease in mass) on the QCM crystal in the first measurement. Once the shipment arrives, further testing on the carrier-free cytokines will be conducted to make sure the change in mass is not from the BSA. However, based on the difference in QCM resonance frequency measurement between the IFN gamma and target-cytokine, TNF alpha, it is safe to assume that the change in resonance frequency is due to the presence of the target cytokine.

	Added material	**Change in resonant frequency (Hz)**
	ug	**Hz**
Nov 11	BSA (50)	+4
Nov 11	BSA (50)	0

Table 5: Effect of BSA on QCM Measurement

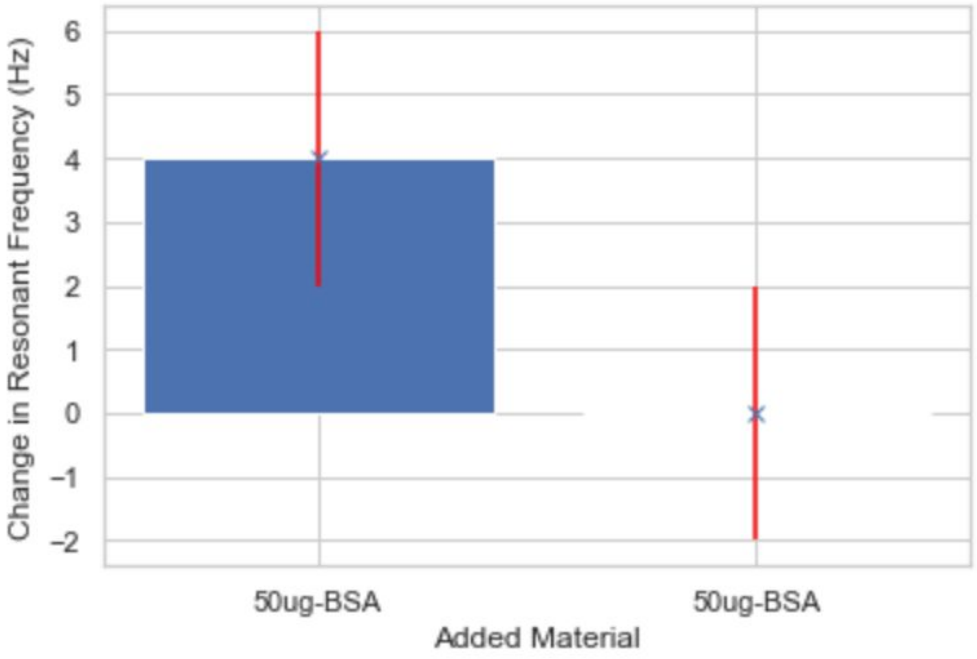

Figure 22: Effect of BSA on QCM Measurement

4.3.1 Fabrication Issue

Some substrates have some small surface stains after the GOPS functionalization step. Washing off unreacted GOPS as soon as substrate is removed from the reaction vial is warranted as there was a thick clear gel-forming on top of the substrate. The staining may be due to using too much reactant material or too long of a reaction time since this problem did not occur for the experiments that used less GOPS. However, these experiments that used fewer reactants also did not have successful functionalization. A fine balance of the concentration and time would need to be further investigated. To get rid of the thick gel, the whole GOPS functionalized substrate was soaked in IPA for a few minutes and the gel was gently pried off along with solution swirling a few times.

The gelling issue is something to get rid of for faster fabrication and a lower chance of breaking substrates by prying off the gel. Based on Wong and Krull, excess moisture will cause GOPS crosslinks and polymerization, which is the gel polymer on top of the QCM crystal substrates when functionalized in the acid-aqueous solvent [43]. To avoid using aqueous-based GOPS functionalization, xylene, and Hunig's base solvent method to functionalize GOPS to silica was employed but the substrate seems to be not successfully functionalized from the aptamer fluorescence test [43]. Again, a concentration, duration, and heat protocol would need to be tested for the successful employment of this method. One thing to note is that the substrate was absolutely gel-free using the xylene and Hunig's method.

Another drawback of the staining from excess GOPS is that the functionalized QCM crystal can not be properly calibrated from the QCM if the staining or residue from GOPS is present as was the case for QCM crystal #4 as shown in the following figure. Normally, the crystal would have sharp peaks at 10, 30, and 50 MHz from calibration. The red line in the figure is the resonance frequency peaks, while the blue line is the dissipation used to find the resonance frequency.

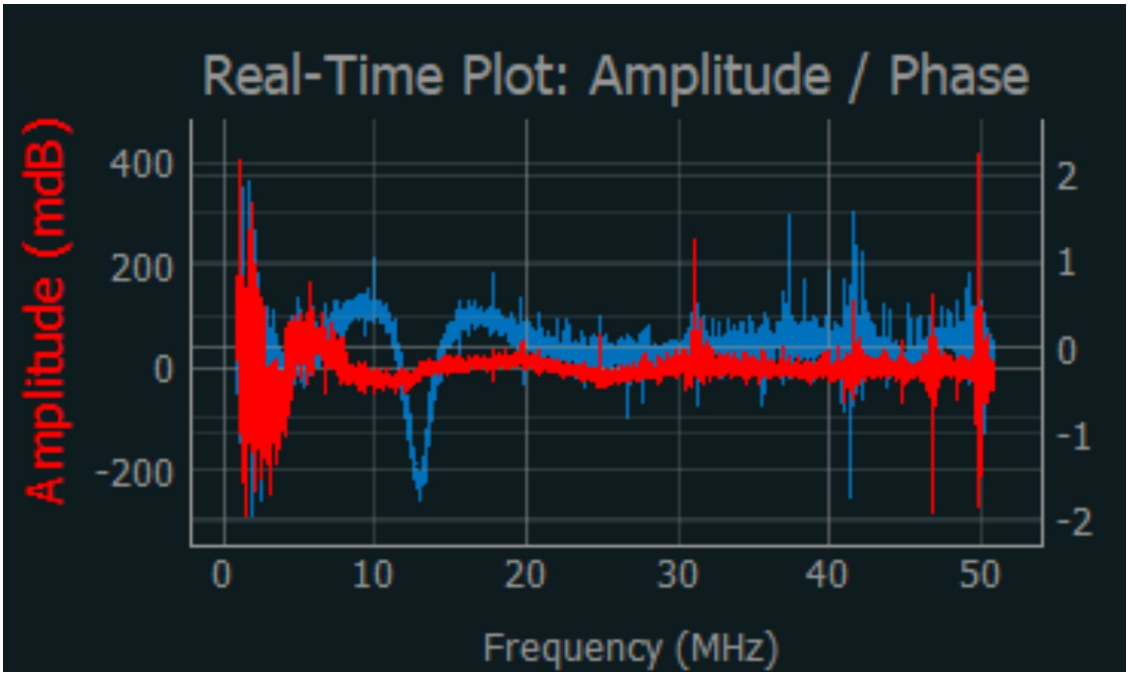

Figure 23: Failed Calibration of 10 MHz QCM Crystal #4's Resonant Frequency

Chapter 5: Conclusion and Future Work

The biosensor was successfully covalently functionalized with silane and amide chemistry using linkers GOPS and CDI. Reducing reactant GOPS concentration and reaction time can remove the GOPS polymerization on the QCM crystal. The sensor fabrication process is reproducible and several quartz crystals showed consistent fluorescence emission change when cytokines have interacted with the substrate. The fluorescence indicates aptamer presence on the substrate and the brightness changes are a result of aptamer shape deformation-induced when target cytokines are bounded.

When interacted with the same concentration of cytokines, the functionalized QCM crystals were responsive to the target cytokines (TNFa) and unresponsive to non-target cytokines (IFNg). This selectivity is important in making reliable biosensors, which will not elicit measurement response on false-positive non-target proteins. Furthermore, the functionalized QCM crystals are reusable, using urea wash to remove aptamer-bounded cytokines, over several weeks.

Covalent functionalization of aptamers is working and can be visualized via the aptamers' fluorescent dye molecules even after 7M urea washing. Results from the mass-based biosensor, QCM, are reproducible, sensitive, and selective to target cytokine. The functionalized QCM crystal-based acoustic sensor also has promising reusability results of 30 to 85%

recoverable sensing surface on subsequent measurement, taken over multiple days or even weeks apart, which shows the robust nature of the biosensor for reusability.

5.1 Future work

XPS characterization will be employed to identify what bonds are present and get direct characterization on the functionalized silica surfaces. The XPS will also be able to confirm if the cytokines are bonded by the sensing layer.

Ultimately, if this sensor were to be used in hospitals for testing cytokines, the biosensor would need to be tested in blood plasma or serum background or saliva rather than PBS buffer for its stability and specificity functionalities. For ease of operation, a microfluidic channel would need to be implemented for fluorescence optical biosensing, 2D sensing layer should be uniformly covered by aptamers, and have a similar-sized substrate (like assay wells) of about 4 cm^2. It would be more ideal to have a pump in place of a syringe for the QCM measurement setup because the bubbles created from the constant emptying of the 3 ml syringe would hinder resonant frequency measurement. The bubbles would need to be flushed out by flowing liquids back and forth. The ridding of bubbles could also displace the target analyte from the O-ring position and added steps will make operations less efficient.

More work needs to be done to find the optimal material and experiment reaction time for the highest coverage / yielding aptamer-based sensing layer. Hopefully, the staining issue can also be resolved under the optimal reaction conditions. Using data analysis of past experimental trials and machine learning models, a script has been made to test for this. Experimental trials of device fabrication would be needed to test the accuracy of the prediction model.

5.2 Novelty of Silane Chemistry and Covalent Linkers Functionalization Method

The covalently functionalized aptamer-based silica sensing layer has the potential to detect a wide variety of small proteins/ molecules. Through SELEX, aptamers can be sequenced to bind to different target molecules. The resonant frequency mechanism employed by QCM and acoustic sensors is sensitive to mass differences down to 0.4 ng [44]. By functionalizing acoustic sensors or QCM crystals with specific aptamers, users can detect target molecules accurately.

In addition, the covalent linkers used in this functionalization rely on silane chemistry. With the use of ALD silica, many surfaces can be functionalized with aptamers to become sensing layers. In regards to functionalizing super stable surfaces such as the TMD 2H phase, the silica ALD method should be applied. Not only would the TMD layer become sensing-capable, but also the expensive and fragile 2D TMD can be passivated.

Moreover, silica is prevalent in the IC industry, the cost of this functionalization should be fairly low. To further cut cost, the fluorescent dyes are not needed for mass-sensitive QCM measurement. Amine linkers used on the aptamers are quite a bit cheaper compared to antibodies and thiol linkers commonly used in QCM crystal or gold functionalization. Lastly, because of the more robust nature of the aptamers compared to antibodies, aptamer-based sensors can be reused; thus, resulting in saved time and resources.

References

[1] K. Kalantar-zadeh, J. Zhen Ou, T. Daeneke, M. S. Strano, M. Pumera, S. L. Gras, “Two-Dimensional Transition Metal Dichalcogenides in Biosystems,” *Advanced Functional Materials,* vol. 25. no. 32, pp. 5086-5099, July 2015.
[2] R. L. Bundea, E. J. Jarvia, and J. J. Rosentreterb, “Piezoelectric quartz crystal biosensors,” *Talanta,* vol. 46, no. 6, pp. 1223-1236, August 1998.

[3] N. Dhenadhayalan, M. I. Sriramc, K. Lin, “Aptamer-based fluorogenic sensing of interferon-gamma probed with ReS2 and TiS2 nanosheets ,” *Sensors and Actuators B: Chemical,* vol. 258, pp. 929-936, April 2018.

[4] J. A. Stenken and A. J. Poschenrieder, ”Bioanalytical chemistry of cytokines – A review,” *Analytica Chimica Acta,* vol. 853, pp. 95-115, Jan. 2015.

[5] Y. Liu, N. Tuleouv, E. Ramanculov, and A. Revzin, “Aptamer-Based Electrochemical Biosensor for Interferon Gamma Detection,” *Analytical Chemistry*, vol. 82. no. 19, pp. 8131-8136, September 2010.

[6] S. D. Jayasena, “Aptamers: An Emerging Class of Molecules That Rival Antibodies in Diagnostics,” *Clinical Chemistry*, Volume 45, Issue 9, pp. 1628-1650, September 1999.

[7] R. A. Potyrailo, R. C. Conrad, A. D. Ellington, and G. M. Hieftje, “Adapting Selected Nucleic Acid Ligands (Aptamers) to Biosensors,” *Analytical Chemistry,* vol. 70, no. 16, pp. 3419-3425, 8 July 1998.

[8] Z. Szekanecz and A. E. Koch, “Successes and failures of chemokine-pathway targeting in rheumatoid arthritis,” *Nature Reviews Rheumatology,* vol. 12, pp. 5-13, 2016.

[9] A. Mantovani, P. Allavena, A. Sica and F. Balkwill, “Cancer-related inflammation,” *Nature,* vol. 454, pp. 436-444, 23 July 2008.

[10] M. C. Cohen and S. Cohen, “Cytokine Function: A Study in Biologic Diversity,”*American Journal of Clinical Pathology,* vol. 105, no. 5, pp. 589-598, 1 May 1996.

[11]*ELISA Technologies IN-HOUSE ANALYTICAL TESTING* (n.d.) [Online]. Available: https://www.elisa-tek.com/support/faqs/.

[12]*ThermoFisher Scientific 96-Well Sample Preparation for Suspension Cells (*n.d.) [Online]. Available: https://www.thermofisher.com/ca/en/home/references/protocols/cell-and-tissue-analysis/elisa-protocol/elisa-sample-preparation-protocols/96-well-sample-preparation-for-suspension-cells.html

[13] M. Gullberg, S. M. Gu´stafsdo´ttir, E. Schallmeiner, J. Jarvius, M. Bjarnegård, C. Betsholtz, U. Landegren, and S. Frediksson, “ Cytokine detection by antibody-based proximity ligation,” *Proceedings of the National Academy of Sciences of the United States of America,* vol. 101, no. 22 pp. 8420-8424, June 2004.

[14] A.V. Lakhin, V.Z. Tarantul, and L.V. Gening, “ Aptamers: Problems, Solutions and Prospects,” *ActaNaturae,* vol. 5, no. 4, pp. 34-43, Oct. 2013.

[15] S. Song, L. Wang, J. Li, C. Fan, and J. Zhao, “Aptamer-based biosensors,” *TrAC Trends in Analytical Chemistry,* Volume 27, Issue 2, Pages 108-117, February 2008.

[16] R. Kong, L. Ding, Z. Wang, J. You, and F. Qu, “A novel aptamer-functionalized MoS2 nanosheet fluorescent biosensor for sensitive detection of prostate specific antigen,” *Analytical and Bioanalytical Chemistry,* vol. 407, pp. 369-377, 2015.

[17] N. Tuleuova, C. N. Jones, J. Yan, E. Ramanculov, Y. Yokobayashi, and A. Revzin, “Development of an Aptamer Beacon for Detection of Interferon-Gamma, ” *Anal. Chem.,* vol. 82, pp. 1851-1857, 2010.

[18] D. Voiry, A. Goswami, R. Kappera, C. C. C. e Silva, D. Kaplan, T. Fujita, M. Chen, T. Asefa, and M. Chhowalla, “Covalent functionalization of monolayered transition metal dichalcogenides by phase engineering,” *Nature Chemistry,* vol. 7, pp. 45-49, 2015.

[19] X. Chen, N. C. Berner, C. Backes, G. S. Duesberg, and A. R. McDonald, “Functionalization of Two-Dimensional MoS2: On the Reaction Between MoS2 and Organic Thiols,” *Angewandte Chemie,* vol. 55, no. 19, pp 5803-5808, May 2016.

[20] R. Huang and R. Huang, Y. Fan and Y. Ling, “Simultaneous Detection of Multiple Cytokines from Conditioned Media and Patient's Sera by an Antibody-Based Protein Array System,” *Analytical Biochemistry,* vol. 294, no. 1, pp. 55-62, 1 July 2001.

[21] S. D. Jayasena, “Aptamers: An Emerging Class of Molecules That Rival Antibodies in Diagnostics,” *Clinical Chemistry,* vol. 45, no. 9, pp. 1628-1650, September 1999.

[22] X. Chen and A. R. McDonald, “ Functionalization of Two-Dimensional Transition-Metal Dichalcogenides,” *Advanced Materials,* vol. 28, no. 27, pp. 5738-5746, July 2016.

[23] C. Backes, N. C. Berner, X. Chen, P. Lafargue, P. La Place, M. Freeley, G. S. Duesberg, J. N. Coleman, A. R. McDonald, “Functionalization of liquid-exfoliated two-dimensional 2H-MoS2”, *Angew Chem. Int. Ed. Engl.,* vol. 54, no. 9, pp. 2638-2642, 2015.

[24] D. Sarkar, X. Xie, J. Kang, H. Zhang, W. Liu, J. Navarrete, M. Moskovits, and K. Banerjee, “Functionalization of Transition Metal Dichalcogenides with Metallic Nanoparticles: Implications for Doping and Gas-Sensing,” *Nano Lett.,* vol. 15, no. 6, pp. 2852-2862, 27 February 2015.

[25] S. Balamurugan and A. Obubuafo, “Surface immobilization methods for aptamer diagnostic applications,” *Anal. Bioanal. Chem.,* vol. 390, no. 4, pp. 1009-21, 23 September 2007.

[26] S. L. Clark and V. T. Remcho, “Electrochromatographic Retention Studies on a Flavin-Binding RNA Aptamer Sorbent,” *Anal. Chem.,* vol. 75, no. 21, pp. 5692-5696, 20 September 2003.

[27] D. Hiller, R. Zierold, J. Bachmann, M. Alexe, Y. Yang, J. W. Gerlach, A. Stesmans, M. Jivanescu, U. Müller, J. Vogt, H. Hilmer, P. Löper, M. Künle, F. Munnik, K. Nielsch, and M. Zacharias, “Low temperature silicon dioxide by thermal atomic layer deposition: Investigation of material properties,” *Journal of Applied Physics,* vol. 107, 29 March 2010.

[28] V. M. Mecea, “Is QCM really a mass sensor,” *Sensors and Actuators A,* vol. 128, pp. 270-277, Feburary 2006.

[29] Deepak, “What are the differences between Raman and IR Spectroscopy?,” 26 June 2016. [Online]. Available: https://lab-training.com/2015/06/26/what-are-the-differences-between-raman-and-ir-spectroscopy/

[30] D. Exline, “Comparison of Raman and FTIR Spectroscopy: Advantages and Limitations,” 09 October 2013. [Online].

[31] B. A. Marrow and A. J. McFarlan, “Infrared and gravimetric study of an aerosil and a precipitated silica using chemical and hydrogen/deuterium exchange probes,” *Langmuir,* vol. 7, pp. 1695-1701, August 1991.

[32] L. T. Zhuravlev, “The surface chemistry of amorphous silica. Zhuravlev model,” *Colloids and Surfaces A: Physicochemical and Engineering Aspects,* vol. 173, no. 1-3, pp. 1-38, 10 November 2000.

[33] A. A. Christy and P. K. Egeberg, “Quantitative determination of surface silanol groups in silica gel by deuterium exchange combined with infrared spectroscopy and chemometrics,” *Analyst,* vol. 130, no. 5, pp. 738-744, 08 April 2005.

[34] J. J. Fripiat, “Silanol Groups and Properties of Silica Surfaces,” *ACS Symposium Series,* vol. 194, pp 165-184, 1 June 1992.

[35] D. Tan, Y. He, X. Xing, Y. Zhao, H. Tang, and D. Pang, “Aptamer functionalized gold nanoparticles based fluorescent probe for the detection of mercury (II) ion in aqueous solution,” *Talanta,* vol. 113, pp. 26-30, 4 April 2013.

[36] M. Jing and M. Bowser, “Methods for measuring aptamer-protein equilibria: A review,” *Anal Chim. Acta.,* vol. 686, pp. 9-18, 10 November 2010.

[37] N. Tuleuova and A. Revzin, “Micropatterning of Aptamer Beacons to Create Cytokine-Sensing Surfaces,” *Cellular and Molecular Bioengineering,* vol. 3, pp. 337-344, 20 November 2010.

[38] K. k. Kanazawa and J. G. Gordon, "Frequency of a Quartz Microbalance in Contact with Liquid," *Anal. Chem.,* vol. 57, pp. 1770-1771, 1 July 1985.

[39] Z. Lin, C. M. Yip, I. S. Joseph, and M. D. Ward, “Operation of an Ultrasensitive 30-MHz Quartz Crystal Microbalance in Liquids,” *Anal. Chem.,* vol. 65, pp. 1546-1551, 1993.

[40] S. J. Martin, V. E. Granstaff, and G. C. Frye, "Characterization of a Quartz Crystal Microbalance with Simultaneous Mass and Liquid Loading," *Anal. Chem.,* vol. 63, pp. 2272-2281, 1991.

[41] M.V. Voinova, M. Jonson, and B. Kasemo, “ ‘Missing mass’ effect in biosensor's QCM applications,” *Biosensors and Bioelectronics,* Volume 17, Issue 10, Pages 835-841, October 2002.

[42] M. Rodahl and B. Kasemo, “On the measurement of thin liquid overlayers with the quartz-crystal microbalance,” *Sensors and Actuators A: Physical,* Volume 54, Issues 1–3, June 1996, Pages 448-456, June 1996.

[43] A. K. Y. Wong and U. J. Krull, ”Surface characterization of 3-glycidoxypropyltrimethoxysilane films on silicon-based substrates,” *Analytical and Bioanalytical Chemistry,* vol. 383, pp. 187-200, August 2005.

[44] "openQCM Sensor Module", Quartz Crystal Microbalance with Dissipation Monitoring: the first scientific QCM entirely Open Source, 2020.